

## Age and Isotope-Geochemical Features of the Murzinka–Adui Metamorphic Complex in Connection with the Problem of Formation of the Murzinka Interformational Granite Pluton

G.B. Fershtater<sup>a,†</sup>, A.A. Krasnobaev<sup>a</sup>, P. Montero<sup>b</sup>, F. Bea<sup>b</sup>, N.S. Borodina<sup>a,✉</sup>,  
M.D. Vishnyakova<sup>a</sup>, N.G. Soloshenko<sup>a</sup>, M.V. Streletskaya<sup>a</sup>

<sup>a</sup> Institute of Geology and Geochemistry, Ural Branch of the Russian Academy of Sciences,  
ul. Akademika Vonsovskogo 15, Yekaterinburg, 620016, Russia

<sup>b</sup> Departamento Mineralogía y Petrología, Campus Fuentenueva, Univ. Granada, 18002, Granada, Spain

Received 6 July 2018; accepted 17 September 2018

**Abstract**—The chemical composition of rocks of the Murzinka–Adui metamorphic complex and the Murzinka granite pluton, a reference interformational granite pluton in the Urals, is considered. A detailed comparative analysis of ancient gneisses and related granite veins included an isotope–geochemical study of zircons from both groups of rocks. Zircons are subdivided into seven age groups (I, 1588 ± 20 Ma; II, 1060 ± 28 Ma; III, 530 ± 11 Ma; IV, 380 ± 6 Ma; V, 330 ± 9 Ma; VI, 276 ± 3 Ma; and VII, 260 ± 3 Ma). The first four groups are apparently zircons from gneisses, reworked to different extents, and the other three groups are zircons crystallized during granite genesis. The gneisses and most of the granite samples contain zircons of all the above age populations, which is evidence of trapping zircons from gneisses by granite melts, on the one hand, and the occurrence of “granite-derived” zircons in gneisses, on the other.

The granitoids and gneisses of all types differ considerably in geochemical features. The behavior of trace elements and the Rb–Sr ages indicate that the formation of granites of the Murzinka massif was a discrete episode of magmatic activity. The Sr isotope ratios in the granites and gneisses indicate different degrees of the mantle–crust interaction and the participation of the material of the crystalline basement and newly formed crust in their formation.

**Keywords:** paragneisses, orthogneisses, granites, protolith, paleocontinental sector of the northwestern megablock, zircon isotope parameters, Rb/Sr age, Middle Urals

### INTRODUCTION

Consideration of the issue reflected in the title of this article was caused by new data on interformational granite plutons of the Urals, which have striking specifics in structure, conditions of formation and metallogeny (Fershtater et al., 2018). Among these plutons Murzinka and Adui are two remarkable granite intrusions, which are famous for rare-metal and semiprecious mineralization. At the base of these plutons are pre-Paleozoic rocks of the crystalline basement of the Ural orogen, at the top—Silurian–Devonian sedimentary–volcanogenic strata, formed predominantly in suprasubduction conditions during the closure of the paleo-oceanic basin. Such a geological position determines many specific structural, geochemical and isotope features of plutons, different from other granite plutons of the similar age in the Urals. In particular, it is possible to trace their role based on the study results of these plutons in the granite genesis in the

pre-Paleozoic folded basement, fragments of which are preserved in the structure of the Ural orogen.

The processes of granite formation in the crystalline basement of mobile belts have been well studied (Kovalenko et al., 1996; Yarmolyuk and Kovalenko, 2003; Slabunov et al., 2006; Tsygankov, 2014). As a large number of studies have been devoted by now to this subject, it should seem that the theme is closed for further detailed consideration. However, this conclusion does not concern such mafic orogens as the Ural orogen and its paleo-oceanic sector, formed during the evolution of the oceanic basin. Until now some researchers deny the very existence of fragments of the crystalline basement within these orogens.

In such fragments of the crystalline basement as the Taratash, Aleksandrovsk, and Ufalei blocks, located in the paleocontinental sector of the Urals, there are no evident signs of formation of large granite plutons and the granite formation is confined by zones of migmatization. Small occurrences of late Paleozoic granite magmatism (Nizhnii Ufalei and some other small granite plutons) show no evident isotope records of their origin within the pre-Paleozoic crust (Shardakova, 2016). The Murzinka–Adui metamor-

<sup>†</sup> Deceased.

<sup>✉</sup> Corresponding author.

E-mail address: gerfer@online.ural.ru (N.S. Borodina)

phic complex (MMC), located on the eastern slope of the Urals in the central part of the Ural orogen has been chosen to study due to extensive development of the magma generation in the crustal conditions resulted in the formation of large granite plutons.

This problem is of special actuality because most granite plutons in the Urals were formed in dome structures (Belavin and Aleinikov, 1968; Trifonov et al., 1968; Fershtater and Borodina, 1975) as a result of diapirism together with crack propagation (Clemens and Mawer, 1992). Such plutons are composed of granitoids with such isotope parameters that indicate that the new crust has played a leading role as a source of granitic melts. This crust was formed as a result of the mantle–crust interaction in the course of the post-oceanic history of development of the Ural orogen (Fershtater, 2013; Fershtater et al., 2018). Most of the whole range of granitoid rocks are characterized by a low primary ratio of  $^{87}\text{Sr}/^{86}\text{Sr} = 0.704\text{--}0.7045$  and positive  $\epsilon_{\text{Nd}}$  values or close to zero. Granites of the interformational plutons have more complex isotope composition reflecting the participation of two sources—crystalline basement and newly formed crust—in their formation.

## RESEARCH METHODS

Analyses were performed at the Analytical Center for Collective Use (“Geoanalitik”) of the Ural Branch of the Russian Academy of Sciences following standard procedures. Rock-forming elements concentrations were determined on SRM-18, SRM-25, and VRA-30 X-Ray fluorescence spectrometers (analysts N.P. Gorbunova, L.A. Tatarinova, and G.S. Neupokoeva) and trace elements on a ICP-MS ELAN-9000 Perkin Elmer mass-spectrometer (analysts D.V. Kiseleva, N.V. Cherednichenko, and L.K. Deryugina). The isotopic composition and concentrations of Rb, Sr, Sm, and Nd were measured with an isotope dilution method on a TRITON Plus (Thermo) multichannel high-resolution mass-spectrometer (analysts N.G. Soloshenko and M.V. Strelets-kaya). The measurement procedure has been considered in detail in (Fershtater et al., 2015).

The age and isotope parameters of zircons were obtained on a SHRIMP-IIe/mc in the IBERSIMS laboratory at the University of Granada (Spain) by professors P. Montero and F. Bea. The measurement procedure is given at [www.ugr.es/~ibersims](http://www.ugr.es/~ibersims). The location scheme of sampling sites in the northern part of the study area is given in Fig. 1.

## COMPOSITION AND STRUCTURE OF THE MURZINKA–ADUI METAMORPHIC COMPLEX

At the latitude of the Murzinka granite pluton 4 types of gneisses are distinguished in the Murzinka–Adui metamorphic complex (MMC).

(1) The western part of the complex is composed mainly of mafic *paragneisses*, interbanding with more silica rocks

(Table 1, ans. 1–4). Banded packets, represented by interchange of biotite, biotite–garnet, biotite–cordierite–sillimanite and tourmaline-bearing biotite–corundum gneisses, are intruded by small granite bodies and pegmatoid granites. These rocks differ from orthogneisses not only in the occurrence of above-mentioned high-alumina minerals, but also in the presence of low-Ti biotite (Table 2, samples 220, 152/50).

(2) The eastern part of the paragneiss zone is composed of *high-alkaline orthogneisses*, similar in composition to alkaline basalts (Table 1, ans. 5, 6), which are well exposed on the Neiva River right bank in the Murzinka village area. Rocks are represented by biotite and clinopyroxene–amphibole–biotite rock varieties containing antiperthitic plagioclase  $\text{An}_{30\text{--}40}$  that is typical of all metamorphic rocks of the Murzinka complex. In comparison to biotite from paragneisses, biotites from orthogneisses ( $\#Mg = 0.48\text{--}0.49$ ) are enriched in  $\text{TiO}_2$ , as well as aluminous amphibole ( $\#Mg = 0.49$ ). Clinopyroxene from these gneisses, as well as from all other varieties of gneisses, is depleted in  $\text{TiO}_2$ ,  $\text{Al}_2\text{O}_3$ , and  $\text{Na}_2\text{O}$  regardless of their nature (Table 2, samples 71, 73). Accessory minerals (magnetite, titanite, apatite, and allanite) are abundant and varied. By chemical composition, these rocks are close to vaugnerites, K-rich basite or diorite rocks common in Variscides of Western Europe (Massif Central, France), which accompany the main phase of the crustal granite formation and reflect the contribution of a mantle source into this process (Sabatier, 1980, 1991; Scarrow et al., 2009). By some researchers, formation of vaugnerites is connected with the most intensive, “catastrophic” melting of the crust (Couzinié et al., 2014).

(3) The central part of the MMC is composed mainly of diorite–granodiorite orthogneisses (Table 1, ans. 7–9), with marble interbeds in places. In the area of the Alabashka pegmatite field (Fig. 1), where many boreholes were drilled during exploration, the section of the central part of the MMC is represented by carbonate rocks (calciphyres), alternating with biotite gneisses of predominantly biotite composition and intruded by veins of granites and adamellites of the Yuzhakovo complex, which constitute preliminary a half of volume of the section (Fershtater, 1994). The metamorphic paragenesis of calciphyres is represented by calcite, dolomite, phlogopite, diopside, and graphite; the mineral composition of gneisses is biotite, amphibole, sometimes diopside and orthopyroxene, orthoclase, antiperthitic plagioclase  $\text{An}_{40\text{--}60}$ , apatite, and magnetite.

Granites intruded into metamorphic rocks crossing their gneissic banding. They contain xenoliths of gneisses and calciphyres metamorphosed under granulite facies conditions. The metamorphic rocks are skarnized at the contact with granite veins. In such places, the development of forsterite, diopside porphyroblasts, bitovnite  $\text{An}_{70\text{--}90}$ , scapolite, and prehnite, as well as chloritization of phlogopite are observed. In addition, there are abundant apatite, titanite, sulfides (pyrite, chalcopyrite). The skarn process is of bimetasomatic type, revealed in granites by the development of prehnite, scapolite, and rarely diopside. The thickness of

endoskarn zones is up to 0.5 m. In contrast to granites, pegmatites of the chamber type (Mokrusha and other veins) have no significant influence on country rocks. They have sharp contacts with country rocks without noticeable changes from both sides.

To the south of the Alabashka pegmatite field, in the Yuzhakovo village area and along the Yambarka River, orthogneisses, varying in the composition from diorite to granitogneisses crop out (Table 1, ans. 10–12). These particular metamorphic rocks, namely widespread in MMC to the

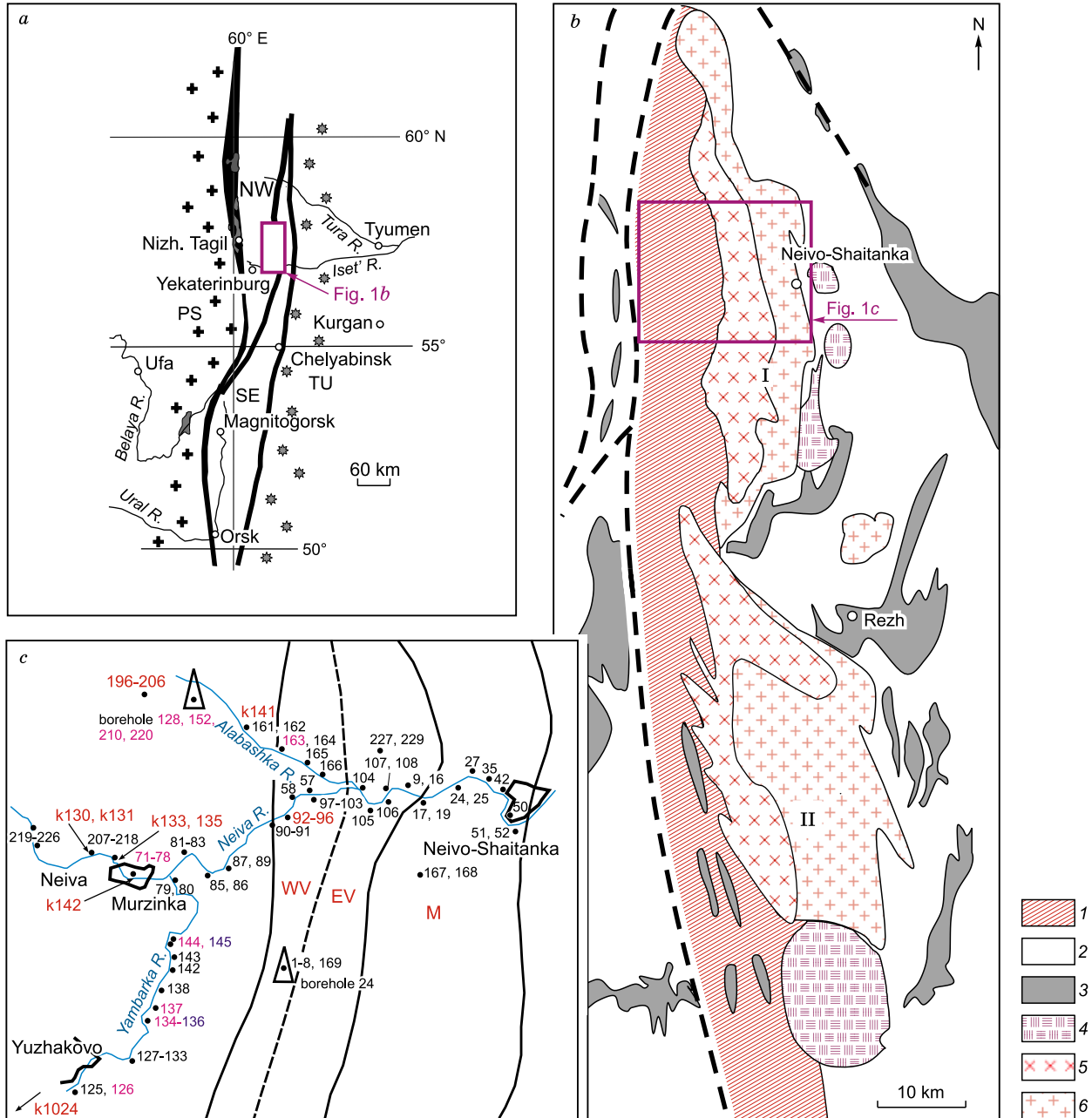


**Fig. 1.** Geological structure of the Murzinka–Adui metamorphic complex and scheme of sampling sites. *a*, Major geological structures of the Urals: PS, paleocontinental sector, TU, Transuralian Region, NW and SE, northwestern and southeastern island arc-continent megablocks (Fershtater, 2013); *b*, geological scheme of the area of Murzinka (I) and Adui (II) plutons, compiled after the Geological Map of the Urals (I.D. Sobolev (Ed.), 1966) with authors' amendments. 1, paragneisses and orthogneisses with marble interbeds, vein granites of the Yuzhakovo complex; 2, Silurian–Devonian volcanosedimentary rocks; 3, serpentinites; 4, Carboniferous tonalites, granodiorites and granites; 5, biotite granites antiperthitic, essentially orthoclase with magnetite, formed due to partial melting of ancient metamorphic formations (Vatikha Complex); 6, two-mica microcline–orthoclase granites, which were originated from the melt, formed at migmatization of Carboniferous tonalites and granodiorites (Murzinka Complex); *c*, location scheme of rock samples of the Murzinka pluton, mentioned in this article. Samples, which yielded zircon ages (with index “k”) and Rb–Sr and Sm–Nd isotope parameters are shown in red; the boundaries of the Murzinka pluton and schematic distribution areas of granites of western Vatikha (WV), and eastern Vatikha (EV) subcomplexes and Murzinka (M) complex are outlined.

**Table 1.** Contents of major (wt %) and trace (ppm) elements in metamorphic rocks of the Murzinka–Adui complex

Ser. No.	1	2	3	4	5	6	7	8	9	10	11	12	13	14	15	16
Sample	k1024	217	220	220/50	73	71	196	210/43	128/22	127	134	144	61	68	93	24/110
SiO <sub>2</sub>	69.7	59.03	67.66	78.3	49.30	55.34	55.38	62.17	66.49	57.17	62.50	70.55	70.15	70.81	68.94	69.00
TiO <sub>2</sub>	0.93	1.16	0.85	0.31	2.31	1.47	0.82	0.71	0.63	0.90	0.98	0.31	0.26	0.24	0.38	0.36
Al <sub>2</sub> O <sub>3</sub>	12.9	21.45	13.25	7.19	17.91	18.19	15.23	14.91	14.35	18.53	16.09	15.90	14.66	15.07	15.34	15.55
Fe <sub>2</sub> O <sub>3</sub>	5.58	2.43	0.70	1.65	2.10	2.15	4.13	1.21	2.56	0.46	2.17	0.40	0.46	0.44	0.35	0.50
FeO	–	1.60	5.60	1.60	8.34	5.23	5.00	4.60	2.80	5.00	3.00	2.47	2.90	1.61	3.58	2.77
MnO	0.06	0.012	0.05	0.05	0.12	0.07	0.156	0.05	0.05	0.10	0.10	0.05	0.05	0.05	0.05	0.04
MgO	2.36	3.05	2.37	1.38	3.52	3.16	5.23	3.61	2.72	3.92	2.64	0.62	0.59	0.47	0.66	1.26
CaO	1.28	0.26	0.48	3.98	5.44	4.52	3.41	3.28	3.11	5.29	4.77	2.50	1.32	1.50	1.50	2.34
Na <sub>2</sub> O	2.61	6.92	2.39	1.52	2.80	4.55	2.95	3.17	3.38	4.40	4.36	4.56	3.67	3.90	4.03	5.00
K <sub>2</sub> O	3.49	3.04	5.30	2.27	3.95	2.75	3.02	4.25	2.41	2.39	2.00	1.51	4.65	4.28	3.65	2.18
P <sub>2</sub> O <sub>5</sub>	0.04	0.01	0.11	0.35	1.21	0.87	0.29	0.32	0.35	0.10	0.31	0.05	0.13	0.10	0.12	0.14
LOI	1.07	0.90	1.00	1.30	2.04	1.22	3.90	1.40	0.80	1.21	0.80	0.27	0.59	0.59	0.39	0.52
Total	100.01	99.87	99.76	99.9	99.04	99.87	99.52	99.68	99.64	99.47	99.71	99.19	99.43	99.06	98.99	99.97
Li	35.93	73.86	125.7	21.07	18.88	30.00	30.53	13.61	10.59	34.00	25.42	20.52	11.26	16.14	16.11	28.00
Rb	156	44.32	73.80	86.94	160.8	149.0	42.38	89.00	75.76	76.00	66.74	53.54	85.54	71.66	67.29	23.00
Cs	3.57	1.05	2.32	1.44	1.83	2.00	2.51	1.65	1.49	3.00	2.05	1.30	0.62	0.56	1.02	1.00
Be	2.70	6.66	1.78	2.98	1.75	3.00	1.05	1.41	1.34	3.00	2.21	2.14	1.67	1.69	1.89	2.00
Sr	246.7	43.82	70.81	95.27	1370	984.6	427.1	272.1	406.1	398.0	345.1	371.8	224.2	427.3	287.7	368.0
Ba	220.8	88.74	185.6	192.2	2527	1830	449.0	667.5	413.1	431.0	358.8	277.5	646.7	1755	1455	468.0
Sc	22.62	22.22	45.24	21.77	13.88	16.00	20.40	12.37	14.37	25.00	14.59	17.57	3.53	2.72	3.46	9.00
V	184.3	605.1	435.0	202.5	250.2	150.0	156.7	74.6	115.7	143.0	102.4	113.1	13.95	28.53	44.79	47.00
Cr	326.2	258.7	191.9	144.9	7.58	3.00	9.78	5.44	37.19	103.0	94.03	70.03	2.97	9.82	17.80	4.00
Co	17.55	39.74	24.80	27.70	17.46	15.00	14.93	12.56	13.82	21.00	16.83	19.38	2.16	3.06	4.67	5.00
Ni	61.96	56.31	57.32	133.1	18.18	18.00	12.77	4.93	22.11	55.00	124.9	47.89	2.44	9.62	14.68	2.00
Cu	9.34	35.19	18.47	765.8	28.87	36.00	142.1	98.78	126.9	8.00	27.81	20.81	7.37	17.73	28.30	28.00
Zn	144.4	29.76	83.68	113.8	140.7	143.0	70.34	73.87	57.18	76.00	64.35	61.98	46.34	71.47	70.50	54.00
Ga	27.49	46.22	33.45	17.87	23.39	16.00	12.96	14.38	14.10	20.00	18.58	18.51	20.26	18.00	19.60	16.00
Y	10.00	1.37	7.95	26.65	23.17	17.90	15.49	15.57	18.79	19.20	16.94	15.56	6.19	1.65	2.18	4.20
Nb	9.69	7.47	2.99	9.58	45.20	62.90	3.61	5.04	4.21	18.20	14.22	11.58	5.98	2.71	4.50	8.50
Ta	0.54	0.31	0.11	0.49	2.12	5.10	0.22	0.31	0.23	2.00	1.00	0.80	0.23	5.47	0.21	0.80
Zr	43.46	227.0	26.06	72.28	28.83	121.0	61.87	50.82	46.12	26.00	21.20	21.25	64.69	105.4	105.2	146.0
Hf	1.27	4.13	0.52	1.31	0.96	1.90	1.94	1.62	1.32	0.80	0.75	0.85	1.90	3.30	3.10	2.60
Mo	0.26	0.17	0.10	2.34	3.56	0.00	0.55	0.74	0.60	0.00	13.18	1.36	0.08	0.97	1.13	0.00
Sn	4.92	1.95	2.37	0.76	3.18	3.30	0.77	0.76	0.54	2.90	2.48	2.56	1.42	1.50	2.35	1.80
Tl	0.94	0.21	2.61	10.36	0.75	0.80	0.87	1.48	0.42	0.40	0.40	5.48	1.18	0.59	0.63	9.60
Pb	8.86	3.45	9.00	6.62	13.71	11.60	11.08	15.41	9.17	11.10	12.41	11.45	28.38	29.21	25.76	19.50
U	11.44	1.74	0.83	2.33	2.21	1.80	2.16	2.21	1.73	0.90	2.03	2.57	1.52	1.19	5.94	2.00
Th	9.9	0.42	1.12	4.78	11.35	15.20	5.00	5.69	4.75	3.00	6.59	4.19	25.50	21.82	17.30	9.00
La	15.15	0.68	5.23	20.36	108.5	59.40	16.83	18.00	19.54	16.50	18.98	19.22	52.36	20.46	22.31	27.70
Ce	27.79	1.65	13.36	39.91	231.7	140.9	34.21	37.46	41.16	34.30	39.09	34.18	88.00	54.16	43.27	48.80
Pr	3.13	0.29	1.90	4.96	21.65	17.20	4.16	4.58	5.23	4.10	4.56	4.62	11.70	4.22	4.81	4.90
Nd	11.44	1.30	8.75	19.11	83.39	67.70	17.01	19.52	22.06	16.30	17.05	17.04	40.32	14.01	16.32	16.40
Sm	2.14	0.35	2.09	3.83	13.45	11.86	3.81	4.24	4.91	3.65	3.52	3.41	6.19	1.92	2.34	2.45
Eu	0.69	0.07	0.38	0.66	3.15	2.91	0.96	1.03	0.96	1.10	1.05	1.13	0.77	0.57	0.67	0.64
Gd	1.93	0.31	1.79	3.60	8.17	8.78	3.67	3.77	4.35	3.46	3.28	3.21	3.57	1.11	1.34	2.08
Tb	0.29	0.05	0.24	0.52	1.00	1.04	0.53	0.54	0.62	0.59	0.53	0.48	0.41	0.11	0.14	0.22
Dy	1.8	0.31	1.30	3.18	5.25	4.21	3.24	3.32	3.77	3.38	3.19	2.99	1.98	0.48	0.64	0.92
Ho	0.36	0.07	0.25	0.66	0.90	0.70	0.67	0.69	0.75	0.73	0.66	0.62	0.33	0.09	0.11	0.16
Er	1.03	0.21	0.73	1.94	2.29	1.72	2.01	1.93	2.14	2.07	1.98	1.81	0.79	0.26	0.34	0.48
Tm	0.15	0.04	0.11	0.28	0.28	0.20	0.29	0.26	0.28	0.33	0.27	0.25	0.09	0.04	0.04	0.06
Yb	0.97	0.28	0.71	1.78	1.60	1.13	1.91	1.59	1.72	1.94	1.83	1.68	0.48	0.22	0.27	0.32
Lu	0.14	0.04	0.10	0.25	0.20	0.13	0.30	0.24	0.25	0.28	0.27	0.25	0.06	0.03	0.04	0.04
W	0.12	7.81	0.30	0.65	0.55	–	0.37	0.66	0.74	–	1.86	0.55	0.09	0.47	1.11	–
Ge	1.66	3.24	2.35	2.08	1.15	–	0.91	0.79	0.90	–	1.02	1.04	0.89	0.70	0.72	–

Note. 1–4, paragneisses; 5–6, high-alkaline orthogneisses; 7–9, orthogneisses of the Alabashka pegmatite field; 10–12, diopside–amphibole–biotite diorite-gneiss and biotite granite-gneiss in the Yuzhakovo village area; 13–16, biotite granite gneisses, which are considered as the restites in western Yuzhakovo granites. Dash, not determined.

**Table 2.** Compositions of rock-forming minerals from gneisses (wt %)

Mineral	SiO <sub>2</sub>	TiO <sub>2</sub>	Al <sub>2</sub> O <sub>3</sub>	Cr <sub>2</sub> O <sub>3</sub>	FeO	MnO	MgO	CaO	Na <sub>2</sub> O	K <sub>2</sub> O	Total	#Mg	An	Ab	Or	<i>n</i>
Biotite–garnet gneiss with cordierite 220																
Bt	35.0	3.37	19.70	0.01	19.30	0.03	8.19	0.00	0.18	9.58	95.36	0.45	–	–	–	3
Kfs	64.8	–	18.90	0.07	0.02	0.04	–	0.06	1.87	13.50	99.33	–	1	16	83	4
Diopside–biotite gneiss with graphite 152/50																
Bt	37.4	1.71	15.30	0.00	15.90	0.33	14.10	0.00	0.10	9.48	94.28	0.62	–	–	–	–
Bt	37.3	2.60	14.50	0.08	16.20	0.37	14.20	0.00	0.07	9.68	94.95	0.62	–	–	–	–
Hbl	49.9	0.29	4.93	0.10	13.40	0.89	13.60	12.30	0.56	0.42	96.38	0.66	–	–	–	–
Cpx	51.5	0.06	1.13	0.00	9.84	1.05	12.40	22.70	0.33	0.01	99.04	0.70	–	–	–	–
Pl	58.0	0.00	26.00	0.00	0.05	0.00	0.00	8.21	7.08	0.37	99.74	–	40	58	2	2
Pl	56.4	0.00	26.80	0.09	0.01	0.00	0.00	9.30	6.49	0.33	99.36	–	45	53	2	–
Diopside–biotite–amphibole gneiss 71*																
Bt	35.9	5.25	12.57	–	20.92	0.39	11.45	0.50	0.16	8.44	95.54	0.49	–	–	–	–
Bt	34.5	4.90	13.04	–	21.56	0.22	11.24	0.56	0.14	8.49	94.87	0.48	–	–	–	–
Hbl	41.6	1.92	10.48	20.76	–	0.43	9.92	11.70	–	–	96.78	0.48	–	–	–	–
Diopside–amphibole–biotite gneiss 134																
Bt	36.5	3.85	14.40	0.07	19.70	0.19	10.70	0.13	0.06	8.59	94.17	0.50	–	–	–	–
Bt	37.0	4.73	13.80	0.03	19.60	0.23	10.80	0.00	0.08	9.40	95.67	0.51	–	–	–	–
Hbl	44.1	1.90	9.58	0.04	17.20	0.38	9.87	11.8	1.43	1.13	97.42	0.51	–	–	–	–
Cpx	51.5	0.12	1.34	0.02	11.40	0.59	11.80	22.5	0.43	0.00	99.63	0.65	–	–	–	–
Pl	61.4	0.00	24.00	0.06	0.03	0.06	0.00	6.02	7.94	0.41	99.93	–	30	67	3	4
Kfs	64.9	0.00	18.40	0.04	0.08	0.00	0.00	0.01	0.90	15.40	99.68	–	0	8	92	2
Kfs	65.3	0.00	18.20	0.06	0.08	0.00	0.00	0.00	0.60	16.00	100.20	–	0	5	95	2
Diopside–biotite–amphibole gneiss 127																
Bt	37.1	3.97	13.80	0.02	17.60	0.21	12.20	0.01	0.03	9.51	94.49	0.56	–	–	–	–
Bt	36.2	4.20	14.40	0.1	18.00	0.12	11.90	0.00	0.05	9.64	94.64	0.55	–	–	–	–
Hbl	43.9	1.41	8.93	0.12	15.80	0.44	11.20	11.7	1.23	1.10	95.77	0.56	–	–	–	3
Cpx	52.3	0.13	1.39	0.00	9.86	0.61	12.40	22.7	0.46	0.00	99.89	0.70	–	–	–	–
Pl	61.4	0.00	24.10	0.01	0.01	0.01	0.00	6.17	8.03	0.50	100.3	–	31	68	3	2
Pl**	61.9	0.03	23.22	0.00	0.07	0.00	0.00	6.02	7.94	0.52	99.67	–	30	68	3	–
Pl**	60.8	0.00	23.80	0.01	0.10	0.00	0.00	6.08	8.29	0.49	99.60	–	30	67	3	–
Kfs**	65.0	0.01	18.03	0.00	0.04	0.00	0.01	0.01	0.84	15.75	–	–	0	9	91	4
Kfs**	64.8	0.00	18.30	0.00	0.02	0.08	0.00	0.00	0.85	15.30	99.33	–	0	8	92	3

Note. Bt, biotite; Hbl, amphibole; Cpx, diopside; Pl, plagioclase; Kfs, K-feldspar; *n*, number of measurements; dash, not determined.

\* Analyses of monofractions of amphibole and biotite in gneiss 71.

\*\* Compositions of plagioclase and K-feldspar in antiperthites from gneiss 127.

south of the Neiva River, they are composed of Ti-rich biotite (#Mg = 0.50–0.56), high-Al amphibole (#Mg = 0.51–0.56), diopside (#Mg = 0.65–0.70), antiperthitic plagioclase An<sub>30</sub>, orthoclase, quartz (Table 2, samples 134, 127), as well as accessory minerals the such as in high-alkaline gneisses, but occurring in a fewer number. It is important that the composition of antiperthites in plagioclase is similar to that of individual K-feldspar grains (sample 127). Hence follows a possibility of the formation of the latter as a result of decay of initially homogenous ternary feldspar that is evidence of high-temperature conditions of the rock formation.

According to the features of the chemical composition, orthogneisses under consideration form the unified genetic and formational group with high-alkaline gneisses.

(4) the very eastern part of the MMC is preserved as *xenoliths in gneisses of the adamellite composition* in the Vatikha granites. These xenoliths represent restites from the process partial melting of the source rocks, what resulted in the formation of granites, which constitute the western part of the Murzinka pluton. The adamellite composition of the restite (Table 1, ans. 13–16) makes it possible suppose the essentially granite composition of the protolith, which have

tasted high degree of partial melting. The characteristic features of the mineral composition of the gneiss restites are the presence of antiperthitic plagioclase  $An_{20-25}$  and orthoclase feldspar.

### Granite veins in MMC gneisses

As it has been noted, the MMC gneisses are intruded by a large number of granite veins varying in thickness from a few centimeters to a few meters, which are united into the Yuzhakovo complex (Fershtater, 1994).

Granitoids of this complex are localized within the metamorphic complex to the west of the Murzinka pluton. They do not form large bodies, but abundant veins of these rocks often predominate in the volume over the enclosed metamorphic rocks.

The early granite veins (the first generation) are represented by gneissic biotite plagiogranites (Table 3, ans. 1–4), which are usually form pygmatic folds (Fig. 2). Rocks are composed of antiperthitic plagioclase  $An_{30-40}$ , quartz, and reddish-brown high-Ti biotite. Rare K-feldspar is represented by orthoclase; accessory minerals are apatite and titanite. The formation of plagiogranites is completed by the development of thin plagiopegmatite segregations as veins and parts in plagiogranites, and then by the development of gneissic or massive granites and adamellites with higher K content, varying in wide limits, reaching 2–3% (Table 3, ans. 3, 4). It should be noted that the orientation of gneissic banding of such veins always coincide with their strike, that is, it seems to be syngenetic. Correspondingly, it has another orientation in relation to plagiogranites of the previous stage.

The granite veins of the second generation represented by biotite granites and adamellites with antiperthitic plagioclase  $An_{30-25}$  and perthitic orthoclase are the most widespread (Table 3, ans. 5–11). It is quite often that rocks have gneissic banding, the orientation of which does not coincide with gneissic banding in veins of the first generation. These relations are repeated in all outcrops and are evidence of

formation of granites of the Yuzhakovo complex in the orogenic conditions; each completed stage of granite genesis, confirmed by the presence of pegmatites, was characterized by their own direction of specific stress. Episodes of tectonic and magmatic activity were congruent. At that, it is necessary to note that all veins of the Yuzhakovo complex represent igneous bodies without noticeable related migmatization (partial melting). Intrusion of the earliest veins of the Yuzhakovo granites was preceded by the development of small quartz–feldspar segregations in gneisses, which is likely to be connected with the partial melting.

The mineral paragenesis of granites was formed under the following  $P$ – $T$  conditions:  $T = 800$ – $650$  °C,  $P = 5$ – $8$  kbar at the ratio of  $P_{H_2O} = 0.5P_{tot}$  (Fershtater, 1994).

### Murzinka pluton

The detailed description of the Murzinka granite pluton and the material composition of granites are given in some works (Fershtater, 1994, 1994, 2013; Fershtater and Borodina, 2018). Let us note that the Murzinka pluton is steeply-dipping to the east with a thickness of about 10 km. The lower part of the pluton is composed of middle Proterozoic rocks of the MMC, the upper part—of Silurian–Devonian volcanosedimentary rocks, metamorphosed under epidote–amphibolite and greenschist metamorphism conditions. The western (lower) part of the pluton is composed of biotite antiperthitic ( $An_{25-20}$ ) orthoclase magnetite-bearing granites of the Vatikha complex. Granites adjacent to metamorphic rocks of the MMC contain xenoliths of more melanocratic rocks of the adamellite composition that are regarded as restites, preserved under a high degree of partial melting, as specified above. Granites—products of such melting—are characterized by definite specificity of the composition and are defined as the western Vatikha subcomplex. These are the very granites which have the most strongly pronounced similarities with the Yuzhakovo granites.

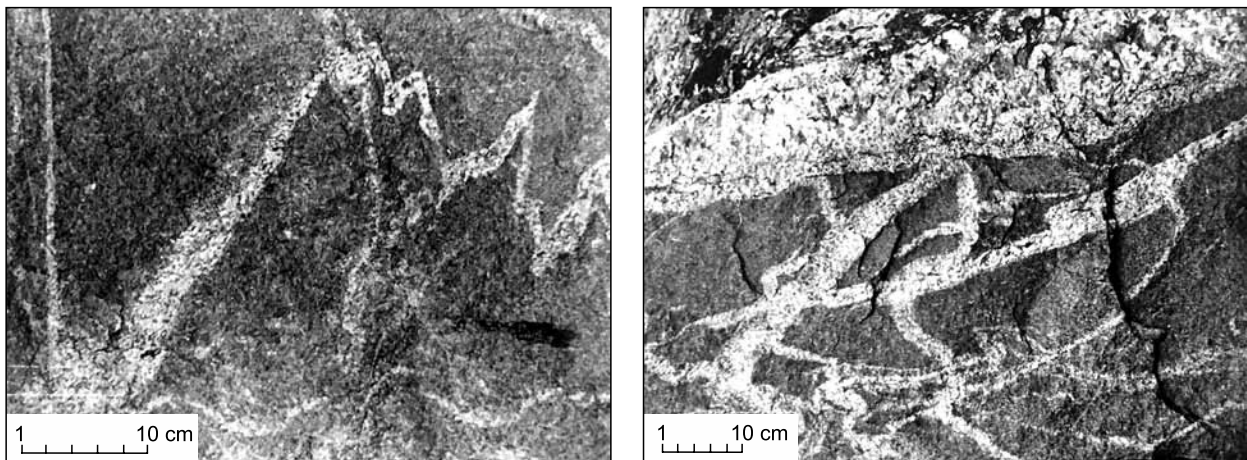


Fig. 2. Photo of vein granites of the Yuzhakovo complex in diorite-gneisses (floodgate near the Yuzhakovo Village).

**Table 3.** Content of major (wt %) and trace (ppm) elements in vein granites

Ser. No.	1	2	3	4	5	6	7	8	9	10	11	12	13	14	15	16
Sample	114	112a	112b	210/50	128/52	152/13	220/38	846	78	122	137	163	k130	k131	k141	k142
SiO <sub>2</sub>	69.81	73.99	72.28	67.40	70.02	71.03	73.39	71.22	72.14	69.58	67.28	72.80	75.49	74.03	68.29	70.40
TiO <sub>2</sub>	0.19	0.08	0.06	0.540	0.67	0.22	0.31	0.17	0.16	0.37	0.92	0.14	0.16	0.19	0.71	0.06
Al <sub>2</sub> O <sub>3</sub>	15.65	15.45	14.09	15.70	13.39	14.73	13.70	15.38	15.10	14.80	16.41	12.39	13.60	13.73	14.04	16.61
Fe <sub>2</sub> O <sub>3</sub>	1.12	0.45	0.53	1.42	2.05	1.08	1.52	0.26	0.17	0.60	0.11	1.08	0.27	0.48	0.55	0.32
FeO	2.55	0.80	3.98	2.10	2.10	0.40	0.40	2.61	1.27	2.66	2.27	1.00	0.72	1.52	3.99	0.75
MnO	0.05	0.05	0.05	0.02	0.02	0.01	0.01	0.05	0.05	0.05	0.05	0.008	0.01	0.04	0.03	0.02
MgO	0.61	0.26	0.24	1.05	1.39	0.32	0.50	0.35	0.38	0.71	0.34	0.27	0.16	0.23	1.42	0.13
CaO	4.19	2.67	1.87	3.34	1.68	1.43	1.25	1.66	1.63	1.65	1.67	1.06	1.34	1.34	1.58	0.48
Na <sub>2</sub> O	3.69	4.56	4.03	4.07	3.17	2.60	2.59	3.12	3.91	3.75	3.35	2.64	3.33	4.03	2.52	3.27
K <sub>2</sub> O	0.69	0.67	2.20	2.92	4.99	5.90	5.83	4.60	3.89	3.73	6.21	6.46	4.64	3.78	5.60	7.05
P <sub>2</sub> O <sub>5</sub>	0.12	0.05	0.05	0.119	0.131	0.061	0.102	0.05	0.05	0.11	0.33	0.063	0.01	0.04	0.36	0.00
LOI	1.01	0.16	0.43	1.20	0.30	2.20	0.40	0.44	0.10	0.63	0.24	1.70	0.21	0.44	0.48	0.83
Total	99.73	99.19	99.81	99.88	99.90	99.98	100.0	99.91	98.85	98.64	99.18	99.63	99.94	99.83	99.57	99.93
Li	13.00	43.45	31.63	18.12	9.87	6.57	13.10	10.07	6.34	31.73	10.00	10.73	9.83	10.04	10.43	1.40
Rb	14.00	2.62	26.27	33.68	83.41	90.21	83.11	48.55	54.10	26.22	95.16	98.08	48.23	74.84	85.80	90.34
Cs	0.00	0.42	0.25	0.30	0.55	0.58	0.29	0.47	0.38	1.36	0.73	0.62	0.35	1.21	0.58	0.27
Be	1.00	9.59	5.24	1.49	1.35	0.76	1.70	0.88	3.08	3.24	1.39	1.32	1.48	1.35	0.49	0.57
Sr	533.0	177.9	283.7	212.6	413.1	304.1	315.7	803.2	623.0	146.4	304.4	216.9	246.1	107.7	285.0	249.2
Ba	78.00	104.4	349.8	1323	1303	2147	2057	1877	1534	990.1	2072	800.2	379.4	359.0	1417	802.8
Sc	10.00	15.89	6.50	4.53	5.03	1.78	6.20	1.14	3.29	5.71	2.63	3.97	1.08	2.56	4.94	0.62
V	20.00	18.48	18.38	44.55	47.90	7.69	23.63	9.00	7.78	55.29	10.49	13.30	9.75	6.34	62.15	3.58
Cr	0.00	22.30	27.44	6.74	4.95	1.11	5.33	3.83	4.80	22.57	1.83	2.05	470.8	7.08	4.71	6.49
Co	2.00	3.44	4.09	5.21	4.90	1.09	3.15	1.40	2.35	6.80	1.68	1.58	5.32	1.92	7.51	1.49
Ni	0.00	32.74	24.39	3.14	2.89	0.95	2.65	3.19	7.72	14.77	2.79	2.20	28.84	8.98	4.92	8.91
Cu	1.00	12.60	50.38	8.50	9.70	7.51	10.62	10.13	9.45	18.06	5.02	5.18	6.19	8.15	95.74	23.06
Zn	27.00	33.85	42.14	86.88	66.58	47.28	90.07	49.59	39.78	97.81	55.89	53.56	19.62	30.68	70.08	24.05
Ga	16.00	39.89	28.51	25.89	20.16	15.17	25.93	15.06	24.06	31.46	17.92	19.81	14.29	15.73	17.59	14.01
Y	8.00	1.61	0.72	1.01	3.61	2.66	3.55	2.17	1.68	1.41	17.97	2.33	0.41	2.22	7.25	0.49
Nb	4.30	4.65	1.38	11.13	7.89	4.12	6.55	0.87	2.50	9.71	5.23	8.80	1.45	6.39	9.30	0.75
Ta	1.90	0.18	0.07	0.22	0.28	0.12	0.11	0.07	0.10	0.27	0.22	0.33	0.03	0.29	0.30	0.04
Zr	14.00	47.21	24.03	140.1	55.28	58.17	355.2	83.77	45.24	271.1	263.9	50.26	43.65	75.61	194.4	22.92
Hf	0.30	1.41	0.60	1.85	1.35	1.26	4.74	2.15	1.74	4.39	7.80	1.67	1.48	2.37	4.21	1.12
Mo	0.00	2.94	1.69	2.31	1.41	1.78	2.14	0.05	0.38	0.51	0.17	0.35	0.57	0.65	0.38	0.76
Sn	0.20	1.61	1.98	0.34	1.18	0.38	0.21	0.53	0.98	2.45	0.72	0.53	0.41	2.11	0.50	0.52
Pb	6.60	15.47	19.14	14.59	16.35	17.62	18.55	22.09	32.08	21.33	43.35	28.21	21.67	29.48	13.05	30.89
U	0.20	0.39	0.44	0.42	1.02	0.56	1.05	1.23	0.66	1.38	3.46	0.72	0.54	1.89	1.35	0.26
Th	0.50	1.98	1.95	2.49	24.74	33.83	13.75	7.53	10.43	6.33	30.51	26.69	1.23	5.27	31.00	0.13
La	5.40	0.58	1.25	3.92	101.6	106.9	36.23	7.61	10.80	5.03	52.41	44.50	4.79	8.22	148.2	1.43
Ce	16.70	1.69	2.48	9.26	184.7	203.3	89.77	16.36	27.40	12.31	135.9	92.61	5.93	15.68	230.3	2.09
Pr	1.50	0.22	0.37	1.03	14.71	16.85	7.22	1.93	2.84	1.24	13.00	9.78	0.87	1.92	26.68	0.22
Nd	6.10	0.95	1.40	3.80	46.62	53.27	23.18	7.40	10.70	4.44	49.54	30.78	2.94	6.94	86.75	0.76
Sm	1.35	0.32	0.34	0.65	5.23	5.92	2.88	1.38	2.10	0.81	10.38	4.09	0.42	1.30	9.94	0.13
Eu	0.68	0.19	0.23	0.19	1.32	1.24	0.49	0.48	0.83	0.22	1.72	1.04	0.28	0.29	1.49	0.50
Gd	1.37	0.34	0.23	0.42	2.29	2.39	1.43	0.86	1.37	0.50	8.12	2.02	0.28	0.96	5.64	0.14
Tb	0.22	0.05	0.03	0.05	0.22	0.22	0.14	0.10	0.15	0.06	1.03	0.19	0.02	0.10	0.33	0.02
Dy	1.31	0.29	0.17	0.27	0.94	0.89	0.66	0.52	0.67	0.28	5.28	0.86	0.09	0.50	1.79	0.09
Ho	0.29	0.05	0.03	0.05	0.14	0.13	0.12	0.09	0.10	0.05	0.91	0.13	0.02	0.09	0.29	0.02
Er	0.86	0.15	0.08	0.12	0.35	0.31	0.29	0.26	0.26	0.13	2.23	0.33	0.04	0.25	0.74	0.05
Tm	0.14	0.02	0.01	0.02	0.04	0.04	0.04	0.04	0.03	0.02	0.26	0.04	0.01	0.04	0.10	0.01
Yb	0.89	0.14	0.08	0.10	0.24	0.18	0.27	0.22	0.17	0.13	1.44	0.25	0.05	0.23	0.59	0.06
Lu	0.14	0.02	0.01	0.02	0.03	0.02	0.04	0.04	0.03	0.02	0.21	0.03	0.01	0.04	0.10	0.01

Granites of the eastern Vatikha subcomplex, located to the east, are significantly more homogenous in composition and mineralogically are close to two-mica orthoclase–microcline (with plagioclase  $An_{12-18}$ ) granites of the Murzinka complex, which constitute the eastern (upper) half of the pluton.

A number of aplitic and pegmatite veins increases close to the top of granite pluton, reaching 50–60% of the total volume. The contacts are of injection type: abundant apophyses of granites, veins of aplites and pegmatite penetrate the country rocks, which underwent strong hydrothermal transformations: mica development, silicification, albitization, and K-feldspathization. The conditions of the granite formation were as follows  $P = 3-4$  kbar,  $P_{H_2O} = P_{tot}$ , crystallization temperature—650–630 °C (Fershtater, 1994).

### Age and isotope parameters

On a SHRIMP-IIe/mc microprobe (University of Granada, Spain), 209 zircon grains from two samples of gneisses (k133 and k1024) and five samples from the Yuzhakovo granite veins (k130, k131, k135, k141, and k142) were investigated (Tables 4, 5). The studied zircons from gneisses and related granite veins are subdivided into seven age groups (Fig. 3): I,  $1588 \pm 20$  (average of 9); II,  $1060 \pm 28$  (6); III,  $530 \pm 11$  (19); IV,  $380 \pm 6$  (19); V,  $330 \pm 9$  (12); VI,  $276 \pm 3$  (67); VII,  $260 \pm 3$  (72). The first four groups include, apparently, zircons from gneisses, reworked to a different extent, another three groups—zircons, which crystallized in the process of granite formation. Zircons of groups I–IV are light in cathodoluminescence, small (usually no more 0.1 mm in size), and isometric contours. Zircons have patchy or sectorial zoning, often corroded, by morphology similar to granulite facies zircons (Krasnobaev, 1986). Zir-

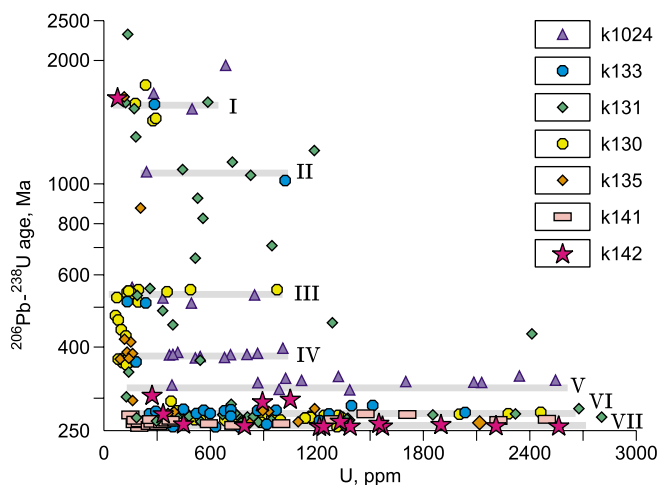


**Fig. 3.** The  $^{206}\text{Pb}/^{238}\text{U}$  age vs. U content diagram in zircons from gneisses and the Yuzhakovo granites. 1, 2, gneisses: 1-k1024, 2-k133; 3–7, granites: 3-k131, 4-k130, 5-k135, 6-k141, 7-k142. I–VII, averaged age dates of corresponding groups of zircons.

cons occur as single separate grains or parts in zonal grains that indicates the discrete transformation of any primary zircon due to events that occurred in the corresponding periods of time. Three young groups of zircons occur as rims or separate grains with well-defined oscillation zoning.

It is important to note that gneisses and the most samples of granites (except for samples k141 and k142) contain zircons of all mentioned age groups (Fig. 3). This is unambiguous evidence of the adoption of “gneiss” zircons in granites, on the one hand, and “granite” zircons in gneisses, on the other hand.

The granites of samples k141 and k142 are the most homogenous and similar in age to granites of the Murzinka pluton (Montero et al., 2000; Gerdes et al., 2002) (Table 4). Dark (U-rich) in CL prismatic zonal grains dominate in them (Fig. 4b), forming two age groups ~280 and 260 Ma. Even in those cases when zircons have light in CL cores, depleted in U and similar in their morphology to those in zircons from gneisses where they have early Paleozoic or Proterozoic ages, there are no age differences between cores and rims. In comparison with zircons from granites of the Murzinka and Adui plutons, which have, as a rule, dark U-rich rims, the rims of zircons from the Yuzhakovo granite veins are often lighter in color (grains 1, 19, and 25 in sample k141 and grain 18 in sample k142 (pegmatoid granite), Fig. 4b). Zircons have magmatic crystal habits and likely crystallized from the granite melt.

Many zircons from granites (samples k130 and k131, Fig. 4a) have light cores (strong cathodoluminescence) with patchy or sectorial zoning. Zircons are subdivided into seven age groups, as mentioned above, each of which (except for the earliest age groups) have both the cores and rims around the younger zircons. Zircons of groups I–III are usually represented by small (up to 0.05–0.07 mm), smoothed isometric crystals, often corroded by later zircon generation. The granite sample k135 contains the well defined zircon groups, represented by light, indistinctly zonal grains, which cement the Mesoproterozoic zircon (1635 Ma). In turn, they are surrounded by rims with an age range of 260–280 Ma.

Biotite–amphibole diorite-gneisses (k133), widespread among country rocks, contain “granite” zircons, which form the same age clusters of 280 and 260 Ma as in granites (Fig. 3, Table 5). They are represented by both single tabular zonal grains and rims around zircons with ages of 1547 and 512–530 Ma (Fig. 5). There are no “granite” zircons of groups VI and VII in biotite gneisses (sample k1024), which occur situated in the western part of the MMC at a significant distance from the Murzinka pluton. Zircons of groups IV and V with the ages of  $385 \pm 4$  and  $332 \pm 3$  Ma, correspondingly, prevail there. The formation of these zircons apparently was connected with impulses of the Paleozoic metamorphism, recorded in rocks of the southern part of the MMC (Vishnyakova et al., 2017; Fershtater et al., 2018). Proterozoic zircons from gneisses belong to groups I–III and form both cores and rims (Fig. 5, gneiss k133, grains 7 and 16). The above-mentioned small rounded grains of the gran-

Table 4. Isotope parameters and ages (Ma) of zircons from granite veins (Yuzhakovo complex)

Group	N	ppm	<sup>208</sup> Pb-corrected isotope ratios			<sup>208</sup> Pb-corrected ages			% dis										
			U	Th	<sup>206</sup> Pb/ <sup>206</sup> Pb ±	<sup>207</sup> Pb/ <sup>235</sup> U ±	Rho	<sup>207</sup> Pb/ <sup>206</sup> Pb ±		<sup>206</sup> Pb/ <sup>238</sup> U ±	<sup>207</sup> Pb/ <sup>235</sup> U ±								
k130 (2.1 km downstream of the Lugovaya Village)																			
VI	19.1	465.5	51.3	17.5	0.11	0.05406	0.001	0.04346	0.001	0.32394	0.009	0.397	373.5	51.2	274.2	4.1	284.9	7	3.8
III	19.2	74.2	54.7	5.6	0.76	0.06044	0.009	0.08615	0.002	0.71791	0.107	0.104	619.5	290	532.7	11	549.4	65.4	3
III–IV	1.2	65.3	39.3	4.4	0.62	0.04436	0.003	0.07619	0.001	0.46597	0.03	0.214	0	0	473.4	8.7	388.4	20.9	21.8
VII	1.1	511.6	82.8	18.7	0.17	0.05411	0.001	0.04222	0.001	0.31496	0.007	0.482	375.7	33.2	266.6	3.6	278	5	4.2
k131 (2.1 km downstream of the Lugovaya Village)																			
I	8	134.6	77.9	50.4	0.59	0.18604	0.004	0.43172	0.008	11.0745	0.322	0.482	2707.5	34.8	2313.5	38	2529.4	27.5	8.6
I	9	114.3	73.2	28.1	0.66	0.10152	0.002	0.28372	0.004	3.97151	0.106	0.388	1652.1	40.8	1610.1	20.6	1628.4	21.9	1.2
I	35	171.3	73.3	39.7	0.44	0.11152	0.002	0.26735	0.005	4.24667	0.104	0.514	1883.1	30	1527.3	23.9	1683.1	20.4	9.2
II	12	529	89.5	70.5	0.17	0.06894	0.001	0.15256	0.003	1.45009	0.038	0.564	896.9	32.8	915.3	17.7	909.9	16	–0.6
II–III	39.3	559.2	201.4	66	0.37	0.05002	0.003	0.1303	0.003	0.89863	0.056	0.27	195.9	130	789.6	17.6	651	30.7	21.2
IV	7	2412	998.9	144.6	0.42	0.05168	0.002	0.06847	0.001	0.48791	0.018	0.314	271.3	73.4	426.9	6.6	403.5	12.3	–5.8
VI	3	184.9	3.8	6.9	0.02	0.05300	0.001	0.0428	0.001	0.31277	0.009	0.585	328.9	37.8	270.2	6.4	276.3	7.2	2.2
VII	15	751.3	174	29	0.24	0.05068	0.005	0.0418	0.001	0.29212	0.028	0.111	226.5	206	264	3.9	260.2	22.3	–1.4
VII	16	870.9	125.4	31.4	0.15	0.05173	0.001	0.04157	0.001	0.29652	0.008	0.416	273.3	52	262.6	4.3	263.7	6.7	0.4
VII	39.1	547.8	86.3	19.8	0.16	0.05288	0.001	0.04183	0.001	0.30494	0.012	0.508	323.5	61.6	264.1	7.1	270.2	9.3	2.2
VII	39.2	296.2	56.3	10.8	0.19	0.05336	0.001	0.04184	0.001	0.30788	0.007	0.389	344.3	45	264.3	3.5	272.5	5.8	3
k141 (former Verkhnyaya Alabashka Village)																			
VI	24.1	1476	121.6	56	0.08	0.05175	0	0.04386	0.001	0.31294	0.005	0.585	274.5	20.2	276.7	3.6	276.5	4	0
VI	24.2	154.6	72.3	5.9	0.48	0.05469	0.002	0.04386	0.001	0.33071	0.016	0.274	399.5	94.6	276.7	4.9	290.1	12	4.6
VII	1	2228	391	80.8	0.18	0.05293	0.001	0.04192	0.001	0.30593	0.007	0.599	325.7	28.2	264.7	5	271	5.6	2.4
VII	19	2495	1599	91.4	0.66	0.05192	0.002	0.04232	0.001	0.30297	0.012	0.267	282.1	80	267.2	3.8	268.7	9.2	0.6
VII	25	311.7	56.2	11.1	0.18	0.05464	0.002	0.04121	0.001	0.31045	0.012	0.449	397.3	67.8	260.3	6.3	274.5	9.6	5.2
k142 (Murzinka Village, right bank of the Neiva River)																			
VII	15	1230.4	140.1	42.8	0.12	0.05172	0	0.04022	0	0.28679	0.004	0.533	272.9	17.6	254.2	2.3	256	2.8	0.8
VII	18	792.6	361.1	28.1	0.47	0.05108	0.001	0.04102	0	0.28892	0.007	0.218	244.7	54.2	259.2	2	257.7	5.8	–0.6
VII	2	1377.3	202.5	47.9	0.15	0.05139	0.001	0.04021	0.001	0.28492	0.007	0.6	258.5	29.6	254.1	5	254.6	5.5	0.2
VII	20.1	1331.9	107.1	48.8	0.08	0.05083	0.001	0.04137	0.001	0.28991	0.008	0.354	233.1	53	261.3	3.4	258.5	6.2	–1
VII	20.2	272.5	30.6	12.9	0.12	0.04804	0.016	0.04201	0.001	0.27823	0.091	0.071	101.1	–	265.3	8.4	249.3	75.2	–6.4

Note. Grains from granite samples k130 19.1, 19.2, and all zircon grains from granite samples k131, k141, and k142 are shown in Fig. 2. In total, 43 grains were measured in sample k130, 44 grains in sample k131, 25 grains in sample k141 and 20 grains in sample 142.

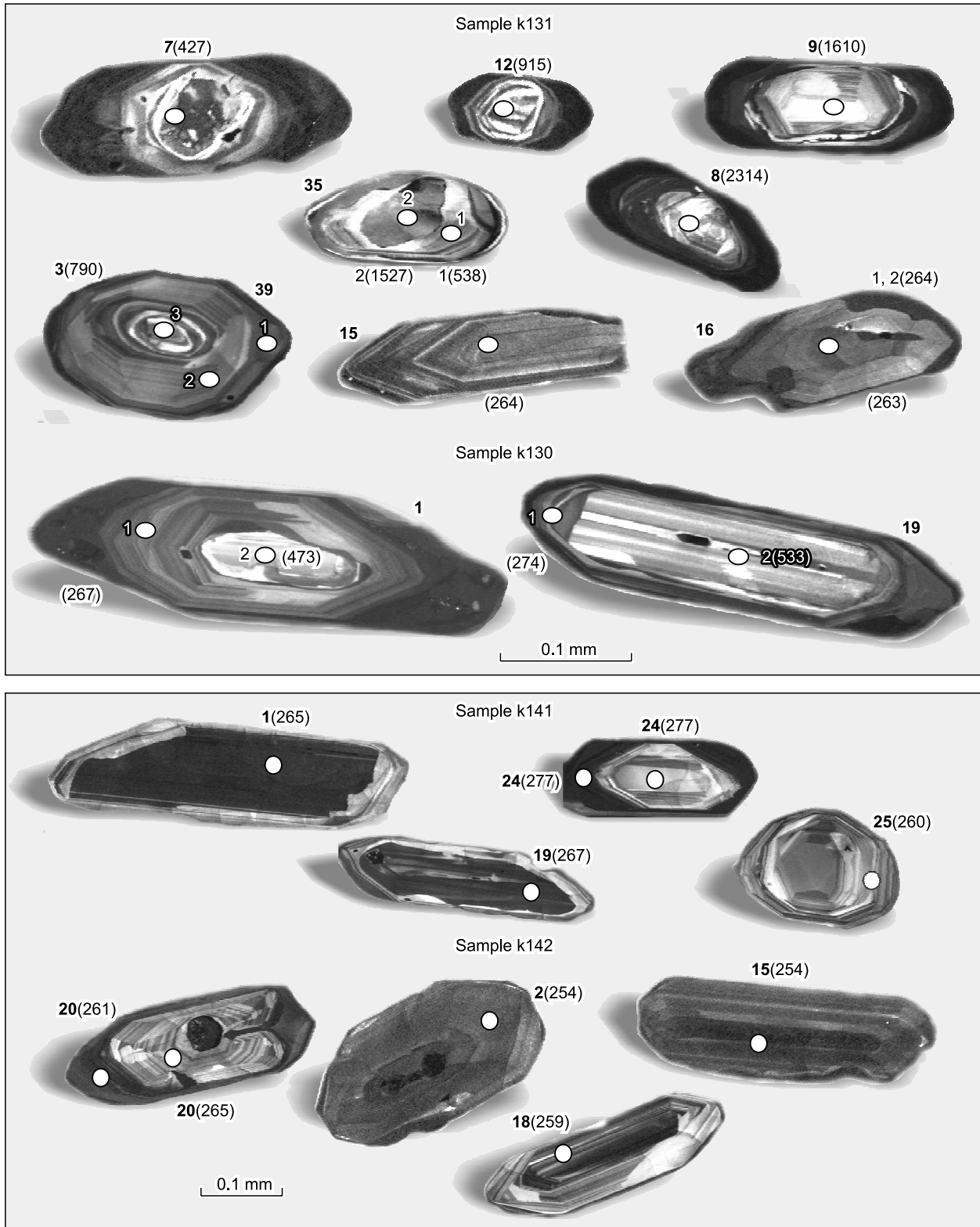


**Fig. 4.** CL images of zircons from granites of the Yuzhakovo complex (k131, k130, k141, k142). Figures—numbers of grains in Table 4, figures in brackets—age, Ma. Measurement points are shown by circles.

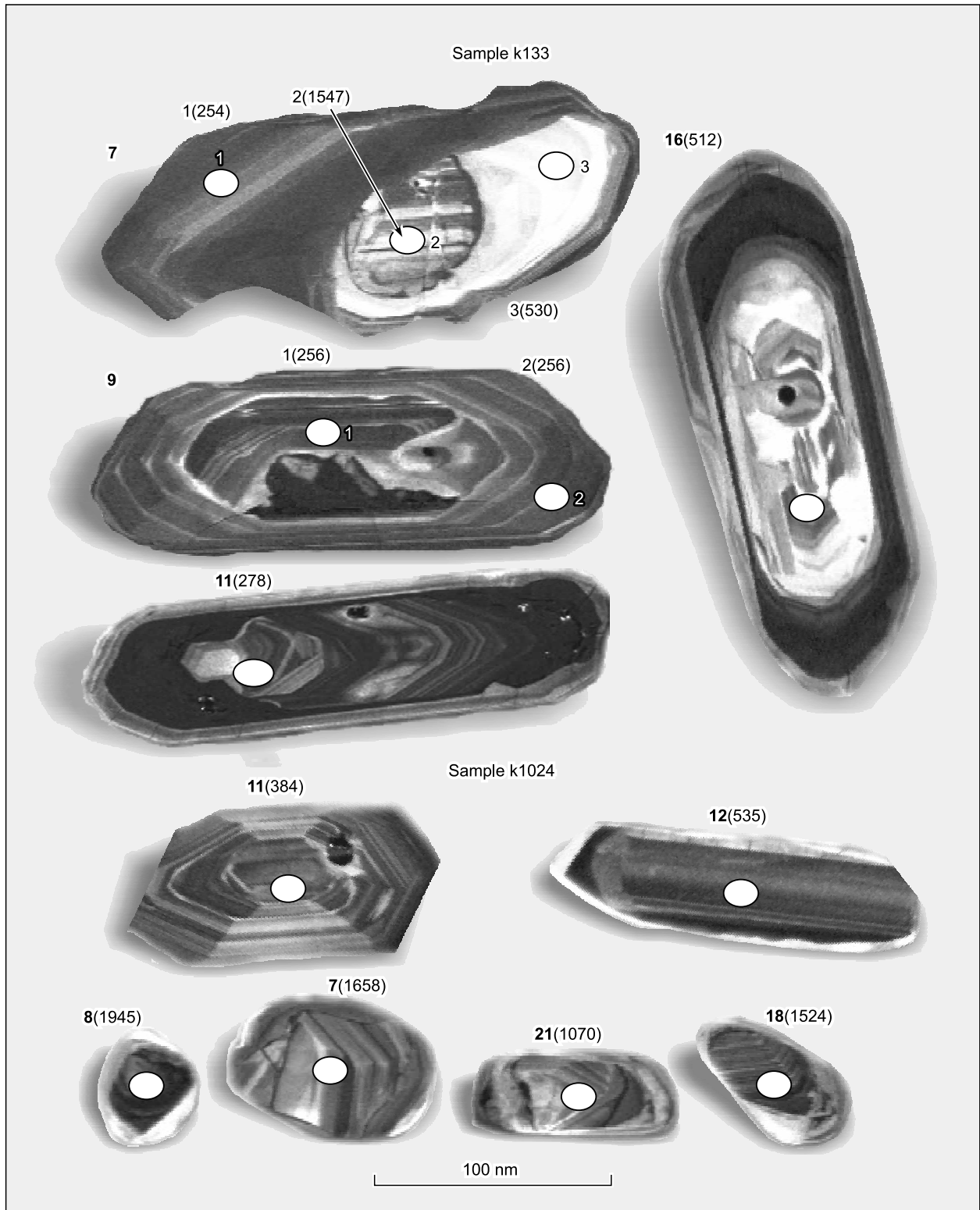


Fig. 5. CL images of zircons from gneisses (k133 and k1024). See legend in Fig. 4.

**Table 5.** Isotope parameters and ages (Ma) of zircons from gneisses of the Murzinka–Adui metamorphic complex

Group	ppm					<sup>208</sup> Pb-corrected isotope ratios					<sup>208</sup> Pb-corrected ages					% dis			
	N	U	Th	<sup>206</sup> Pb	Th/U	<sup>207</sup> Pb/ <sup>206</sup> Pb	±	<sup>206</sup> Pb/ <sup>238</sup> U	±	<sup>207</sup> Pb/ <sup>235</sup> U	±	Rho	<sup>207</sup> Pb/ <sup>206</sup> Pb	±	<sup>206</sup> Pb/ <sup>238</sup> U		±	<sup>207</sup> Pb/ <sup>235</sup> U	±
k1024 (the dam in the Byzovo Village)																			
I	8	687.1	320.6	209.8	0.48	0.12091	0.001	0.35224	0.005	5.87213	0.111	0.573	1970	19.2	1945	25.4	1957	16.5	0.6
I	7	280.5	62.5	71.6	0.23	0.10269	0.001	0.29338	0.004	4.15404	0.083	0.536	1673	23.6	1658	21.8	1665	16.5	0.4
I	18	498	218.4	115.1	0.45	0.09415	0.002	0.26675	0.004	3.46289	0.075	0.464	1511	30.2	1524	19.1	1519	17.3	−0.4
II	21	240.1	66.2	37.6	0.28	0.08538	0.002	0.18053	0.007	2.12521	0.096	0.576	1324	51.4	1070	35.9	1157	31.8	7.6
III	12	849.6	207.2	63.8	0.25	0.05609	0.001	0.08658	0.002	0.66958	0.020	0.455	456	51	535	9.9	521	12.5	−2.8
IV	16	866.9	395.8	46.4	0.47	0.05477	0.001	0.06181	0.001	0.46684	0.013	0.318	403.1	53.8	386.6	4.5	389	8.9	0.6
IV	11	714.3	228.2	37.9	0.33	0.05292	0.001	0.06131	0.001	0.44738	0.010	0.411	326	39	384	4.6	375	6.8	−2.2
IV	1	806.1	236.1	42.9	0.3	0.05418	0.001	0.06145	0.001	0.45904	0.009	0.464	378.5	31.8	384.5	4.7	383.6	6.2	−0.2
IV	13	370.3	94.3	19.7	0.26	0.05384	0.001	0.06143	0.001	0.45602	0.009	0.423	364.3	33.6	384.3	4.2	381.5	6.1	−0.8
V	29	1025	604.8	51.1	0.56	0.05307	0.001	0.05293	0.001	0.38733	0.010	0.293	331.9	54.4	332.5	3.6	332.4	7.7	0
V	25	867.7	495.4	39.4	0.59	0.05339	0.003	0.05244	0.001	0.38605	0.020	0.309	345.3	103	329.5	7.2	331.5	14.9	0.6
k133 (western outskirts of the Murzinka Village)																			
I	7.2	284.1	58.5	66.6	0.21	0.16075	0.004	0.2713	0.008	6.01334	0.242	0.528	2464	45.2	1547	40.7	1978	35.7	22
III	7.3	133.3	68.7	9.9	0.53	0.05771	0.003	0.08565	0.002	0.68145	0.035	0.343	519	95.8	530	12.4	528	21.4	−0.4
VII	7.1	383.6	132.8	13.4	0.36	0.05143	0.001	0.04015	0.000	0.28473	0.007	0.338	260	49	254	2.9	254	5.6	0.2
III	16	202.3	163.6	14.4	0.83	0.06	0.003	0.08259	0.002	0.68332	0.038	0.235	604	111	512	9.1	529	23.4	3.2
VI	10	1397	297.3	55.3	0.22	0.05164	0.001	0.04572	0.000	0.32552	0.007	0.374	269.3	38.8	288.2	3	286.1	5.1	−0.8
VI	5	870.5	200.2	34.1	0.24	0.05206	0.001	0.04517	0.001	0.32427	0.008	0.526	288.1	36.4	284.8	4.9	285.2	6	0.2
VI	11	730.3	158.2	27.8	0.22	0.05302	0.001	0.04399	0.001	0.32156	0.007	0.477	330	33.4	278	3.7	283	5.1	2
VI	15	572.3	57.9	21.9	0.1	0.0514	0.001	0.04409	0.000	0.31248	0.007	0.361	258.7	40.4	278.2	2.9	276.1	5.1	−0.8
VII	9.1	626.8	89.9	22	0.15	0.05132	0.001	0.04052	0.000	0.28673	0.005	0.39	255	35.8	256	2.6	256	4.4	0
VII	9.2	741.3	178	26	0.25	0.05114	0.001	0.04046	0.001	0.28528	0.006	0.506	247	32	256	3.6	255	4.5	−0.4
VII	21	4404	171.1	163	0.04	0.05048	0.000	0.04111	0.001	0.28615	0.004	0.659	217.1	10.2	259.7	3.3	255.5	3.2	−1.6
VII	7	383.6	132.8	13.4	0.36	0.05143	0.001	0.04015	0.000	0.28473	0.007	0.338	260.1	49	253.8	2.9	254.4	5.6	0.2

Note. % dis =  $(^{207}\text{Pb}/^{205}\text{U} - ^{206}\text{Pb}/^{208}\text{U}) / ^{207}\text{Pb}/^{205}\text{U} \cdot 100$  for all grains is less than 3, except for k1024-21 (7.6) and k133-7.2 (22). The measurement points of zircons from gneiss samples k1024 11, 12, 18, 21, 7, and 8 and from gneiss samples k133 11, 16, 7\_1, 7\_2, 7-3, 9\_1 and 9\_2 are shown in Fig. 4. In total, 30 zircon grains were measured in sample k1024 and 25 grains in sample k133.

ulite habit are widespread in gneisses (Fig. 5, gneiss k1024, grains 7, 8, 18, 21).

The distribution of zircons measured points relative to the concordia line in  $^{206}\text{Pb}/^{238}\text{U} - ^{207}\text{Pb}/^{235}\text{U}$  diagrams and calculations of age dates of different clusters of zircon grains from granites and gneisses are given in Figs. 6 and 7, correspondingly.

The study results of zircons from gneisses testify that the ages obtained recorded different stages of rock transformation, while the presence of Mesoproterozoic zircons indicates, apparently, the corresponding age of gneisses by themselves. The presence of age and morphological groups of zircons in granite veins, similar to those in enclosing gneisses is evidence of xenogenic origin of zircon age groups I–III, on the one hand, and of joint epoch's formation of zircon groups IV–VII, on the other.

In addition, the Sm/Nd age dates of gneisses and granite veins of the Yuzhakovo complex (Table 6, Fig. 8) record, seemingly, certain intermediate formation stages of rocks,

which cannot be interpreted reliably. The Rb/Sr age of orthogneisses of group III, which dominate in the central part of the MMC is  $923 \pm 17$  Ma at the primary ratio of  $^{87}\text{Sr}/^{86}\text{Sr} = 0.70037 \pm 0.00013$  (Fig. 8). The  $\epsilon_{\text{Nd}}(1000)$  value varies from 5 to 20, which together with the low content of radiogenic Sr indicates the mantle source of gneisses. The isotope parameters of granites vary widely, but samples, collected approximately at the same sampling site (boreholes drilled within the Alabashka pegmatite field), give an isochron with age of  $457 \pm 9.8$  Ma and isotope ratio of  $^{87}\text{Sr}/^{86}\text{Sr} = 0.71110 \pm 0.00012$ . The similar high primary Sr isotope ratio consistent with the negative  $\epsilon_{\text{Nd}}$  value (Table 6, Fig. 9) and the data previously obtained for granites of the western part of the Murzinka pluton (Montero et al., 2000; Gerdes et al., 2001) indicate a source with high value of  $^{87}\text{Sr}/^{86}\text{Sr}$  contributed to the granite formation. Such  $^{87}\text{Sr}/^{86}\text{Sr}$  value was not recorded neither in gneisses and enclosing rocks nor rocks of the newly-formed crust of the Ural orogen (Fershtater, 2013). It may be assumed that the pre-Pa-

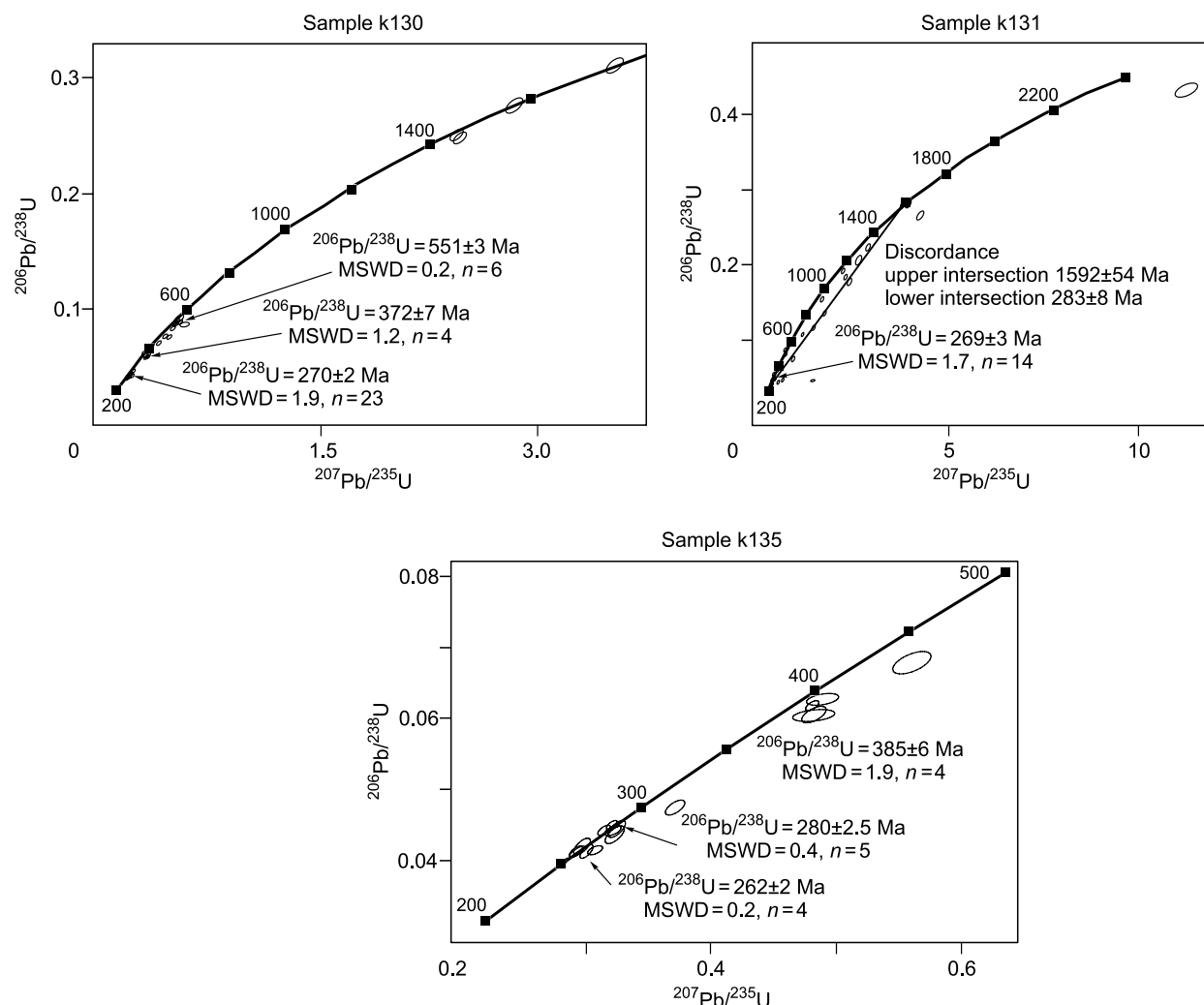


**Fig. 6.** The concordia diagram  $^{206}\text{Pb}/^{238}\text{U}$ – $^{207}\text{Pb}/^{235}\text{U}$  for zircons from granites. Discordia line for sample k130 by points of 2.1, 21.1, 39.3, and 10.1.

leozoic silica rocks exposed by erosion only in the easternmost zone of the MMC, adjacent to granite plutons were a source of both granite veins and granites of the western part of the Murzinka pluton. The host gneisses can be considered to be the protolith only for some granite veins of the first generation with a low content of  $^{87}\text{Sr}/^{86}\text{Sr}_{\text{init}}$  (for example, sample 129 in Fig. 10).

The bimodality of young zircons from the Yuzhakovo gneisses and granites is similar to that recorded in zircons from granites of the Adui pluton (Fershtater, 2013) and reflects the stages of granite formation, which are characterized by the presence of two major stages of 280–290 and 260–255 Ma.

The detailed isotope study of the Murzinka pluton (Montero et al., 2000; Gerdes et al., 2002) demonstrated its heterogeneity: granites of the Vatikha complex are characterized by a high content of radiogenic Sr ( $^{87}\text{Sr}/^{86}\text{Sr}_{\text{init}} = 0.7093$ ), while it is much lower ( $^{87}\text{Sr}/^{86}\text{Sr}_{\text{init}} = 0.7042$ ) in granites of the Murzinka complex (Fig. 10). The  $\epsilon_{\text{Nd}}^{255}$  value varies widely: from –11.9 to –0.05 for the Vatikha

complex, from –8.9 to +4.1 for the Murzinka complex. K–Ar, Rb–Sr,  $^{207}\text{Pb}$ – $^{206}\text{Pb}$  and U–Pb ages of granites of the same complex are in a range of 248–259 Ma. At this, the most reliable zircon age dates lie in a narrow age range of 250–255 Ma, which is accepted as the age of rocks. The isotope composition of granites of the Murzinka pluton testify that there were two sources of their formation: gneiss granites of the MMC adjacent from the west, which served presumably as a source of the Yuzhakovo granite veins, for the Vatikha granites and rocks of the newly-formed crust of the Ural orogen adjacent from the east for the Murzinka granites.

### Geochemistry

The geochemical features of the rocks are rather evident (Tables 1, 2). The highest concentrations of nearly all trace elements were observed in high-alkaline gneisses (Fig. 11). All gneisses are characterized by the ratio  $\text{La}/\text{Yb} > 1$ , minimum for paragneisses and maximum for high-alkaline

Table 6. Rb–Sr and Sm–Nd parameters of gneisses and granites

Sample	Rb, ppm	Sr, ppm	$^{87}\text{Rb}/^{86}\text{Sr}$	$\pm 2\sigma$	$^{87}\text{Sr}/^{86}\text{Sr}$	$\pm 2\sigma$	$^{87}\text{Sr}/^{86}\text{Sr}_i$	$(\epsilon_{\text{Sr}})_i$	Nd, ppm	Sm, ppm	$^{147}\text{Sm}/^{144}\text{Nd}$	$\pm 2\sigma$	$^{143}\text{Nd}/^{144}\text{Nd}$	$\pm 2\sigma$	$\epsilon_{\text{Nd}_i}$	$^{143}\text{Nd}/^{144}\text{Nd}_i$
Gneisses																
73	158.41	1355.2	0.3382	0.0034	0.707306	0.000014	0.702470	-12.11	88.61	14.55	0.09926	0.00001	0.512289	0.000005	5.7	0.511637
196	5.45	55.03	0.2863	0.0029	0.706880	0.000014	0.702785	-7.62	33.52	4.66	0.08412	0.00001	0.512348	0.000007	8.8	0.511796
144	59.16	408.30	0.4191	0.0042	0.705901	0.000013	0.699907	-48.55	17.88	4.51	0.15255	0.00001	0.512106	0.000006	-4.7	0.511105
134	74.72	376.46	0.4701	0.0057	0.706542	0.000019	0.699819	-49.80	15.81	4.01	0.15343	0.00001	0.512888	0.000006	10.4	0.511881
210/43	104.64	335.37	0.9031	0.0090	0.712224	0.000028	0.699309	-57.06	24.63	3.94	0.09681	0.00001	0.513034	0.000017	20.6	0.512398
220/50	72.1817	72.6472	2.8783	0.0001	0.72060	0.000002	0.679394	-340.2	24.71	4.93	0.12060	0.00001	0.512684	0.000009	10.7	0.511892
93	114.41	415.04	0.7015	0.0080	0.709698	0.000016	0.699666	-51.98	20.75	3.74	0.10902	0.00001	0.512722	0.000014	12.9	0.512006
Granites																
116	25.61	612.90	0.1208	0.0012	0.704518	0.000009	0.704102	-2.08	5.49	1.15	0.12709	0.00004	0.512625	0.000010	2.4	0.512375
846	10.33	97.94	0.3050	0.0005	0.705800	0.000001	0.704449	4.3	19.96	3.17	0.09587	0.00001	0.512691	0.000014	2.4	0.512530
163	140.1	259.4	1.5635	0.0156	0.715234	0.000013	0.709562	76.13	96.07	10.99	0.06916	0.00001	0.511746	0.000004	-12.5	0.511610
137	121.4	410.6	0.8561	0.0086	0.717597	0.000021	0.714491	146.12	160.78	26.35	0.09910	0.00001	0.511734	0.000004	-13.9	0.511539
152/13	138.0	386.8	1.0330	0.0103	0.717679	0.000024	0.713932	138.18	143.10	15.05	0.06358	0.00000	0.511606	0.000003	-15.0	0.511482
220/38.5	133.0	374.6	1.0279	0.0103	0.717740	0.000011	0.714011	139.30	125.99	13.87	0.06656	0.00001	0.511695	0.000005	-13.4	0.511564
128/52.2	90.0	435.9	0.5979	0.006	0.714892	0.000014	0.712723	121.01	59.69	6.84	0.06926	0.00001	0.511756	0.000006	-12.3	0.511620
122	118.98	404.70	0.8515	0.0085	0.717887	0.000020	0.714252	145.30	57.80	7.23	0.07565	0.00002	0.511470	0.000004	-18.2	0.511321
210/50	121.76	388.69	0.9071	0.0091	0.716891	0.000015	0.713018	125.97	44.63	6.19	0.08389	0.00002	0.511574	0.000005	-16.4	0.511409
126	164.68	405.26	1.1789	0.0118	0.735698	0.000019	0.730665	376.58	14.54	2.14	0.08880	0.00001	0.511604	0.000014	-16.1	0.511429
78	96.80	860.12	0.3257	0.0004	0.710000	0.000001	0.708606	63.3	18.08	3.30	0.11045	0.00001	0.511795	0.000008	-13.2	0.511578

Note.  $^{87}\text{Sr}/^{86}\text{Sr}_i$ ,  $(\epsilon_{\text{Sr}})_i$  and  $^{143}\text{Nd}/^{144}\text{Nd}_i$ ,  $(\epsilon_{\text{Nd}})_i$  were recalculated in terms of age 1000 Ma for gneisses and 300 Ma for granites.

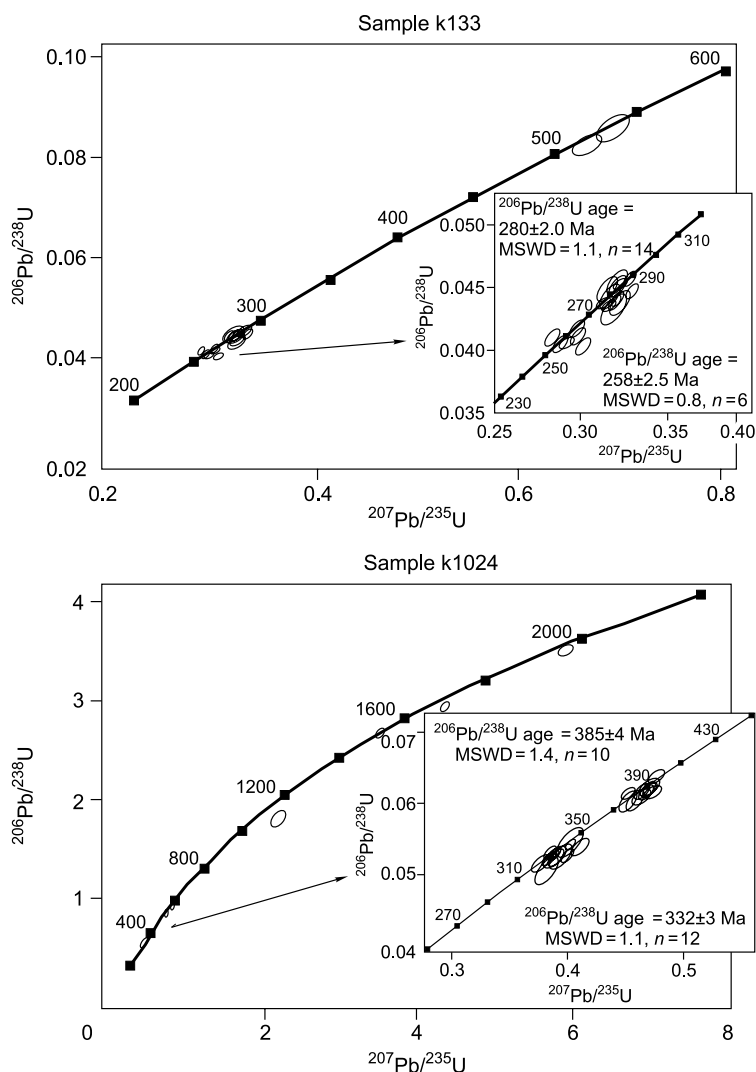


Fig. 7. The concordia diagram  $^{206}\text{Pb}/^{238}\text{U}$ – $^{207}\text{Pb}/^{235}\text{U}$  for zircons from gneisses of samples k133 and k1024.

gneisses. Diorite gneisses, which are widespread in the MMC, show the similar trend but lower (2–3 times) concentrations of Sr, Nd, Nb, LREE in comparison with high-alkaline gneisses. Evidently, these groups of rocks form a unified association. In addition, some geochemical features of rocks of the western part of the MMC are of importance: low concentrations of Sr, Ba, Y, Pb, Th, LREE and higher concentrations of Li, Ga, Ge, as well as Cr, V, Co. Gneisses under consideration are different from the most Paleozoic rocks of the Urals by the presence of positive anomalies of Pb and Li (Fershtater, 2013).

The geochemical distinctions are observed between granites of the Yuzhakovo complex, forming numerous vein bodies, on the one hand, and granites of the Vatikha and Murzinka complexes being made up the unified Murzinka pluton, which formed during the uniform granite-forming process, on the other hand. The figurative points of the Vatikha and Murzinka granites do not form the general trend, but occupy the compact field that can be due to the contamination of granites with the material of enclosing gneiss-

es (that is evident from the occurrence of zircons captured from gneisses in granites) and the diversity of the substratum and a high temperature of magma generation, providing the variations in the degree of melting. In particular, the latter explains the lower  $\text{SiO}_2$  content in some Yuzhakovo granites, great variations in the  $\text{SiO}_2$  content in comparison with granites of the Vatikha and Murzinka complexes (Fig. 12). An insignificant positive correlation between contents of Sr and Ba and  $\text{SiO}_2$  is recorded in granite veins of the second generation, but the Nb content shows the negative correlation with  $\text{SiO}_2$ . There are no correlation links between Rb, Y, Zr, and  $\text{SiO}_2$ . The positive correlation between K and Rb is well marked (Fig. 13). The Yuzhakovo granites are characterized by higher K/Rb ratio, equal to 500.

In contrast to the Yuzhakovo granites, the Murzinka ones form a clear geochemical trend which coincides with the spatial one—from west to east within the Murzinka pluton concentrations of Rb, Li, and Nb in granites increase, while concentrations of Ba and Sr decrease (Fig. 14). These trends do not coincide with the field of the Yuzhakovo granites

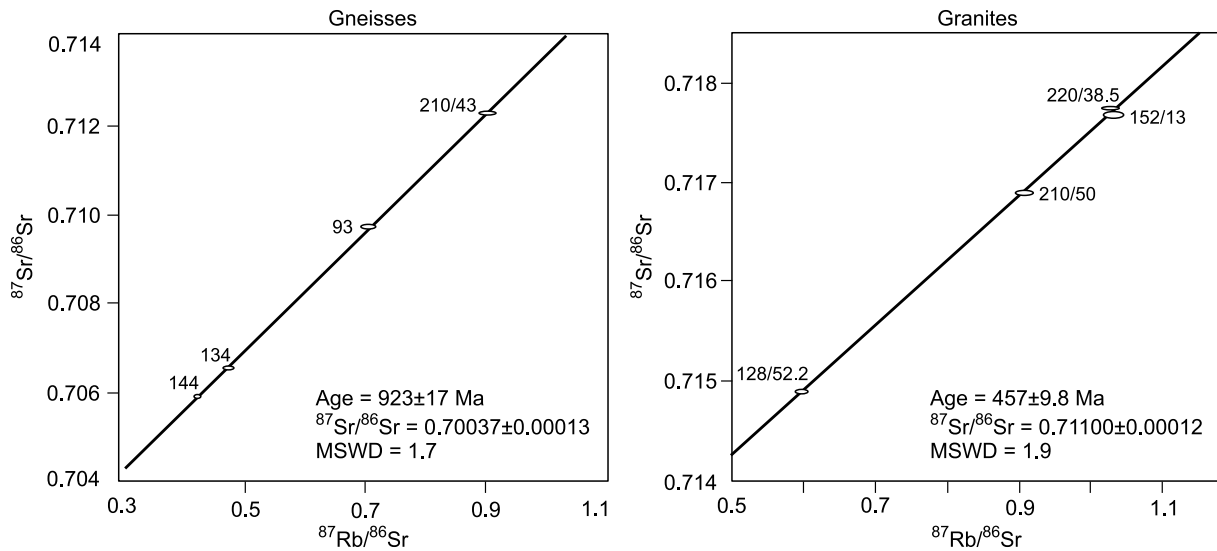


**Fig. 8.** The  $^{87}\text{Sr}/^{86}\text{Sr}$ – $^{87}\text{Rb}/^{86}\text{Sr}$  diagram for gneisses and granites of the Yuzhakovo complex. Chemical compositions of rocks are given in Tables 1 and 3, isotope parameters—in Table 5.

points. Only the points of the adjacent western Vatikha granites lie usually in the field of the Yuzhakovo granites. These granites have the same higher K/Rb ratios.

It is evident that the formation of the Murzinka pluton represents the separate episode of magmatism that is confirmed by a gap between Rb/Sr ages of granites forming Murzinka pluton and Yuzhakovo granites apart from distinct geochemical data. As a result, we deal with not only varying morphology of melt localization (veins, on the one hand, and a large pluton, on the other), but with the material composition of rocks and their petrological and geochemical features. The Yuzhakovo granites correspond to a deeper, higher-temperature and less aqueous stage of magmatism in comparison with granites of the Murzinka pluton.

## DISCUSSION

At the foot of the Murzinka pluton—the reference interformational pluton in the Ural orogeny—there are Mesoproterozoic gneisses of varying composition, at the top—Paleozoic volcanogenic–sedimentary rocks. Such a geological position determines many features of the material composition of rocks, the structure of the pluton and its metallogeny.

Four rock associations are distinguished among gneisses: paragneisses (1), mafic orthogneisses of higher alkalinity (2), diorite- and granodiorite gneisses, alternating in places with calciphyres and marbles (3), and granite gneisses (4). Rocks are metamorphosed under granulite facies conditions and intruded by numerous veins of granites of the Yuzhakovo complex.

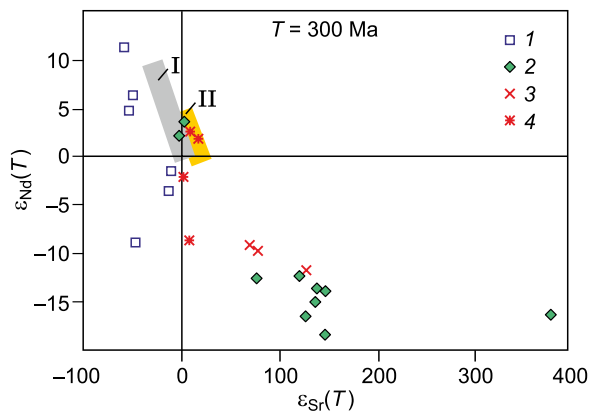


**Fig. 9.** The  $\varepsilon_{\text{Nd}}(300)$ – $\varepsilon_{\text{Sr}}(300)$  diagram for rocks of the Murzinka pluton and its western frame. 1, 2, gneisses (1) and vein granites of the Yuzhakovo complex (2); 3, 4, granites of the Vatikha (3) and Murzinka (4) complexes, constituting the Murzinka pluton. Solid lines I and II represent mantle (I) and mantle–crust (II) evolutionary trends of granitoids of the Urals.

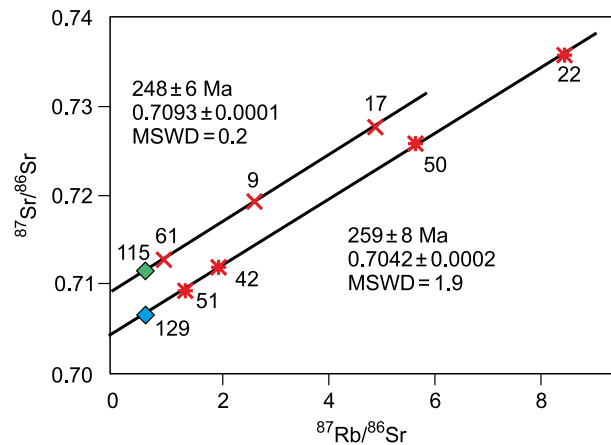


**Fig. 10.** Diagram  $^{87}\text{Sr}/^{86}\text{Sr}$ – $^{87}\text{Rb}/^{86}\text{Sr}$  for granites of the Vatikha (oblique crosses) and Murzinka (asterisks) complexes. Samples 129 and 115 represent the Yuzhakovo granites of I and II generations (Montero et al., 2000).

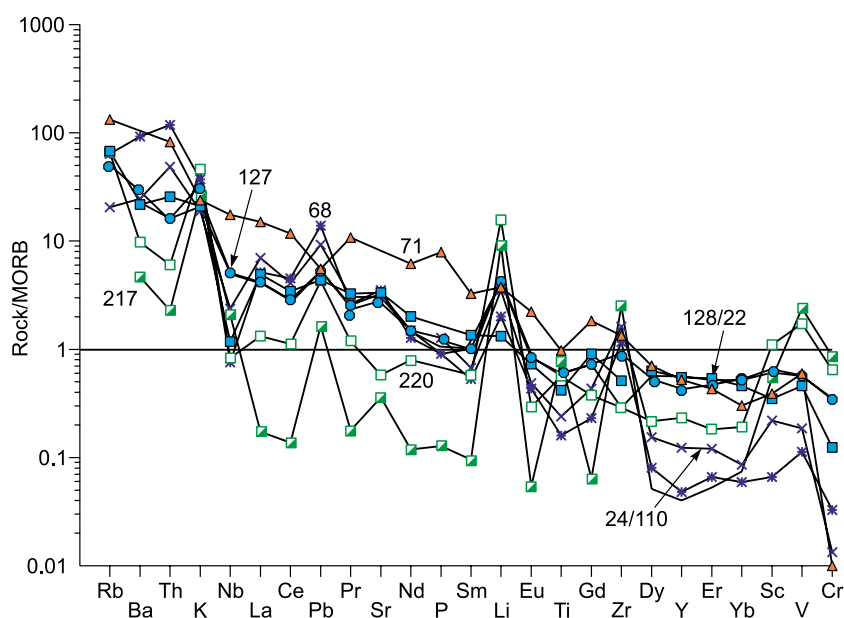


Fig. 11. Distribution of rare-earth and trace elements in the MMC gneisses. Numbers of samples correspond to those in Table 1.

The studied zircons from gneisses and granite veins (Tables 4, 5) are subdivided into seven age groups (Fig. 3): I,  $1588 \pm 20$  (average of 9); II,  $1060 \pm 28$  (6); III,  $530 \pm 11$  (19); IV,  $380 \pm 6$  (19); V,  $330 \pm 9$  (12); VI,  $276 \pm 3$  (67); VII,  $260 \pm 3$  (72). The first four groups include, apparently, zircons from gneisses, reworked to a different extent; the last three groups—zircons, which were formed during the process of granite formation.

The Rb/Sr age of orthogneisses of group III, which dominate in the central part of the MMC, is  $923 \pm 17$  Ma at the primary ratio  $^{87}\text{Sr}/^{86}\text{Sr} = 0.70037 \pm 0.00013$  (Fig. 8). The  $\varepsilon_{\text{Nd}}(1000)$  value varies from 5 to 20 that together with low concentration of radiogenic Sr indicates the mantle source of gneisses. The isotope parameters of vein granites ( $^{87}\text{Sr}/^{86}\text{Sr} = 0.71110 \pm 0.00012$ ,  $\varepsilon_{\text{Nd}} = -12 \div -18$ ) at the age of about 460 Ma, in contrast, indicate that the source of granites had high  $^{87}\text{Sr}/^{86}\text{Sr}$  content. Neither gneisses and enclosing granites, nor rocks of the newly formed crust of the Ural orogen do not possess such  $^{87}\text{Sr}/^{86}\text{Sr}$  value. One can assume that the pre-Paleozoic silica rocks exposed by the erosion only in the easternmost zone of the MMC adjacent to granite plutons can be considered as a source of granite veins. The occurrence of no evident migmatization and intrusive contacts of veins testify that the generation zone of granitic melts of the Yuzhakovo complex was located below the recent erosion level. The wide variations in the composition of granitoids of the Yuzhakovo complex are much more significant than those of granites of the Vatikha and Murzinka complexes, which constitute the Murzinka pluton. It seems to be due to variations in a degree of partial melting and the composition of the protolith.

Granites of the Vatikha and Murzinka complexes made up the western and eastern parts of the Murzinka pluton,

correspondingly. In the endocontact zone (up to 1–1.5 km wide), Vatikha granites contain inclusions of granodiorite and adamellite composition, which represent restites of the granite–gneiss substratum reworked to a different extent. These granites, distinguished as the western Vatikha subcomplex, are similar in by the chemical composition and mineralogy to the Yuzhakovo granites. To the east, they are gradually enriched in Rb, Li, and Nb and defined as the eastern Vatikha subcomplex. By all parameters, the Vatikha granites are similar to those of the Murzinka complex. In addition, they are characterized by clear “crustal” isotope characteristics, while the Murzinka granites are highly different for the latter in low concentration of radiogenic Sr and  $\varepsilon_{\text{Nd}}(255)$  values close to zero. Taking into account the fact that granites have similar isotope ages, these data clearly show that the Vatikha and Murzinka granites had different protoliths. The presence of abundant gneiss–granite inclusion in the Vatikha granites enables us to explain isotope parameters of granites by the fact that Proterozoic gneissic granites were the substratum of the Vatikha pluton. At this, isotope parameters of the Murzinka granites and their spatial proximity to Paleozoic sedimentary–volcanogenic units suggest that rocks of the newly-formed crust of the Ural orogen, common for the most of granites of the Urals, were the protolith of the Murzinka pluton (Fershtater, 2013).

The different composition of the protolith of western lower and eastern upper parts of the Murzinka pluton at preliminary the same age of magma generation and, correspondingly, granites determined well-defined features of the structure of the Murzinka pluton and associated ore mineralization. From west to east, the composition of granites comes nearer to minimum water-saturated granite eutectics: the An content of plagioclase decreases from  $\text{An}_{25-30}$  to  $\text{An}_{12-18}$ , an-

tiperthites disappear, biotite granites are changed by two-mica ones, concentrations of Rb, Li, and Cs in biotite increase (Fershtater, 1994), and a number of pegmatite segregations and granite veins increase. All these features reflect the in-

crease in the water saturation of the granitic magma in the upper part of the pluton, the increase in  $P_{H_2O}/P_{tot}$ , and the decrease in temperature. Moreover, they indicate the leading role of the fluid differentiation at the emplacement of the

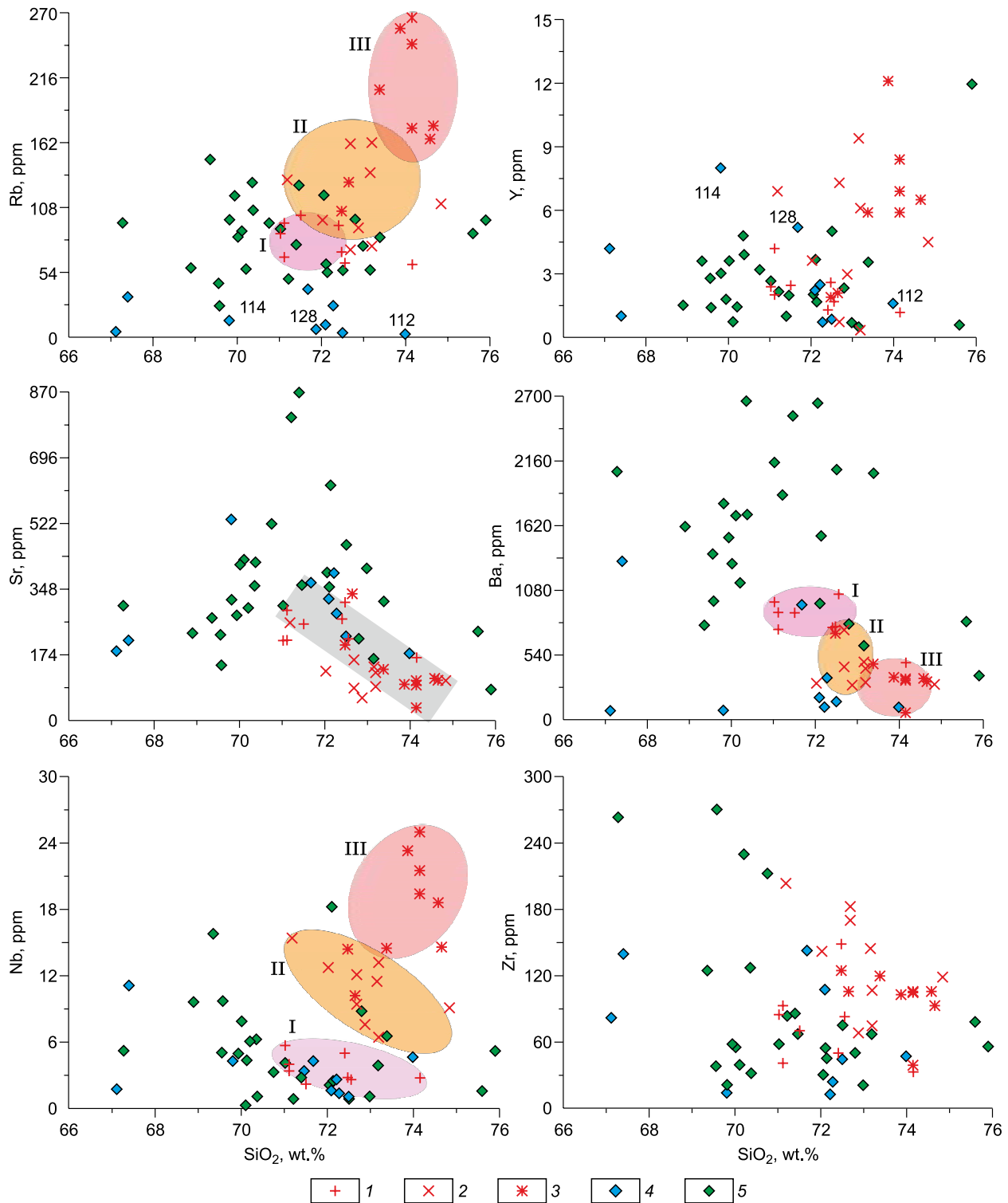


**Fig. 12.** Diagrams  $SiO_2$ –Rb, Y, Sr, Ba, Nb, Zr in granites. 1–3, granites of the Murzinka pluton: western Vatikha (1) and eastern Vatikha (2) subcomplexes, Murzinka complex (3); 4, 5, Yuzhakovo complex, veins of the first (4) and second generations (5). Ovals with corresponding numbers designate fields of granites of the Murzinka pluton. The trend of the Yuzhakovo granites is shown by gray line.

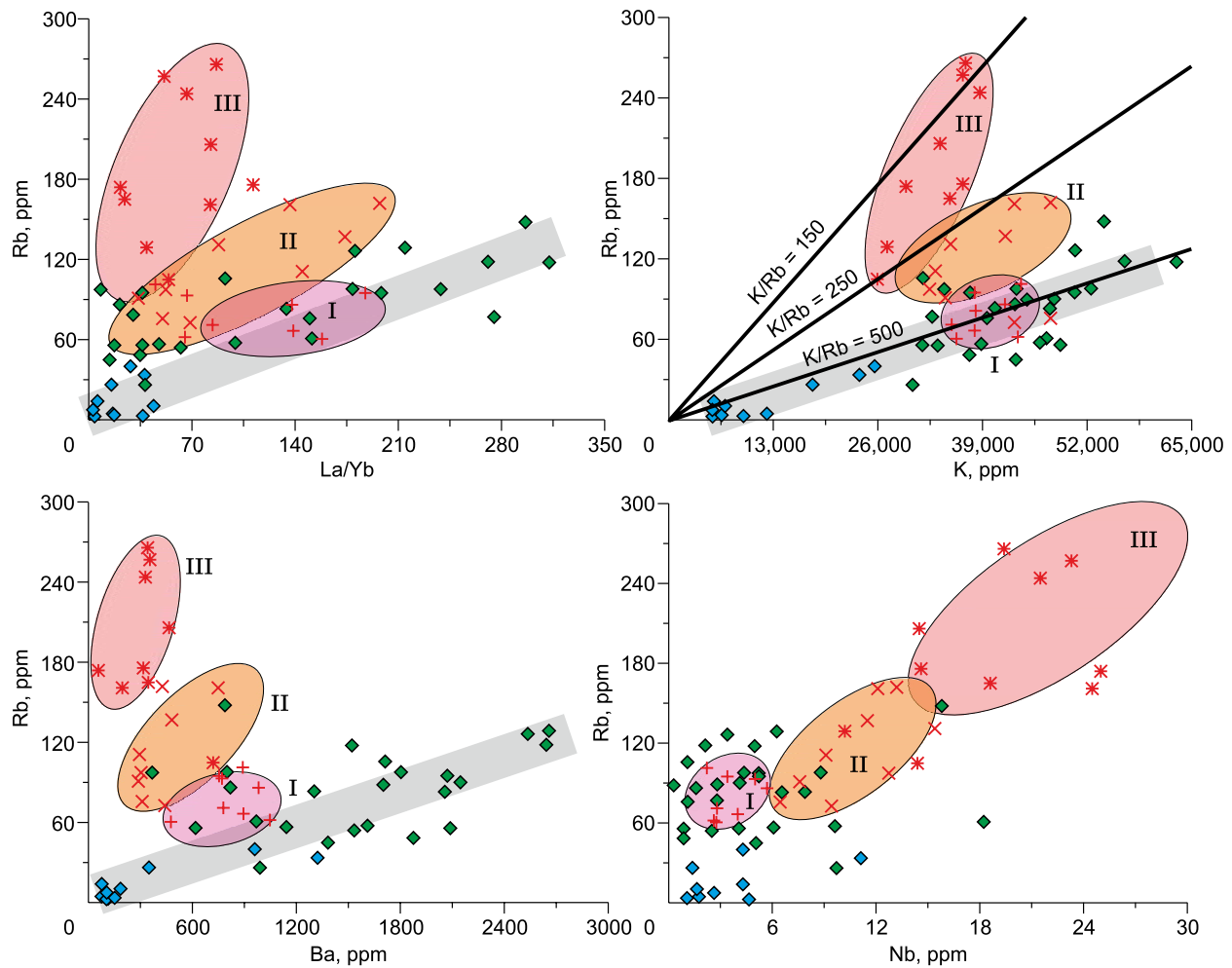


Fig. 13. Diagrams Rb–La/Yb, K, Ba, Nb. See legend in Fig. 12.

Murzinka pluton. This is confirmed by the distinct geochemical zoning (Figs. 13 and 14), recorded in the increase in concentrations of such “fluid” elements as Rb, Li, and Nb in the upper part of the pluton, as well as by the development of metasomatic rare-metal (Mo, Li, Be) mineralization in the top and the upper exocontact. This mineralization is the most widespread in the Adui pluton and the southern continuation of the Murzinka pluton.

$P$ – $T$ – $H_2O$  parameters of the evolution of granite magmatism are shown in Fig. 15. Based on the position of figurative points of granites of different complexes in the Ab–An–Or diagram, taking into account the known data on the temperature relations of feldspar compositions (Ribbe, 1975; and references therein), one can estimate approximately the temperature of their crystallization, which drops from 750 °C for granites of the Yuzhakovo complex to 650 °C for granites of the Murzinka complex.

The evolutionary trend fixes the regular change of the  $P$ – $T$  parameters of the granitoid complexes formation through the latitudinal section of the pluton, that is, from the bottom to the top, from granitoids of the Yuzhakovo com-

plex to the Murzinka granites. The pressure at derivation of eutectic granite melt varies from 6–7 to 3 kbar, and the water fluid content in the melt increases from 4–5 to 8 wt %. The points of the Murzinka granites lie at the granite liquidus curve near the stability curve of muscovite in the granite melt that is in accordance with two-mica composition of granites.

The granitic melt filled the fault zone (strike-slip fault) at the boundary between the pre-Paleozoic basement in the west and the newly-formed crust, composed of Silurian–Devonian volcanogenic-sedimentary rocks in the east, predominantly following the dike emplacement mechanism (Petford et al., 1993). The latter is confirmed by the subvertical shape of granite bodies varying in structure and composition within the Vatikha and Murzinka complexes (Fershtater, 1994). The above features of the Murzinka granite pluton are characteristic in varying degrees for the majority of the Permian granite plutons of the paleocontinental zone of the northwestern megablock, and differ from granites of the Kochkar anticlinorium, where coeval granites of the paleocontinental zone of the southeastern megablock are most

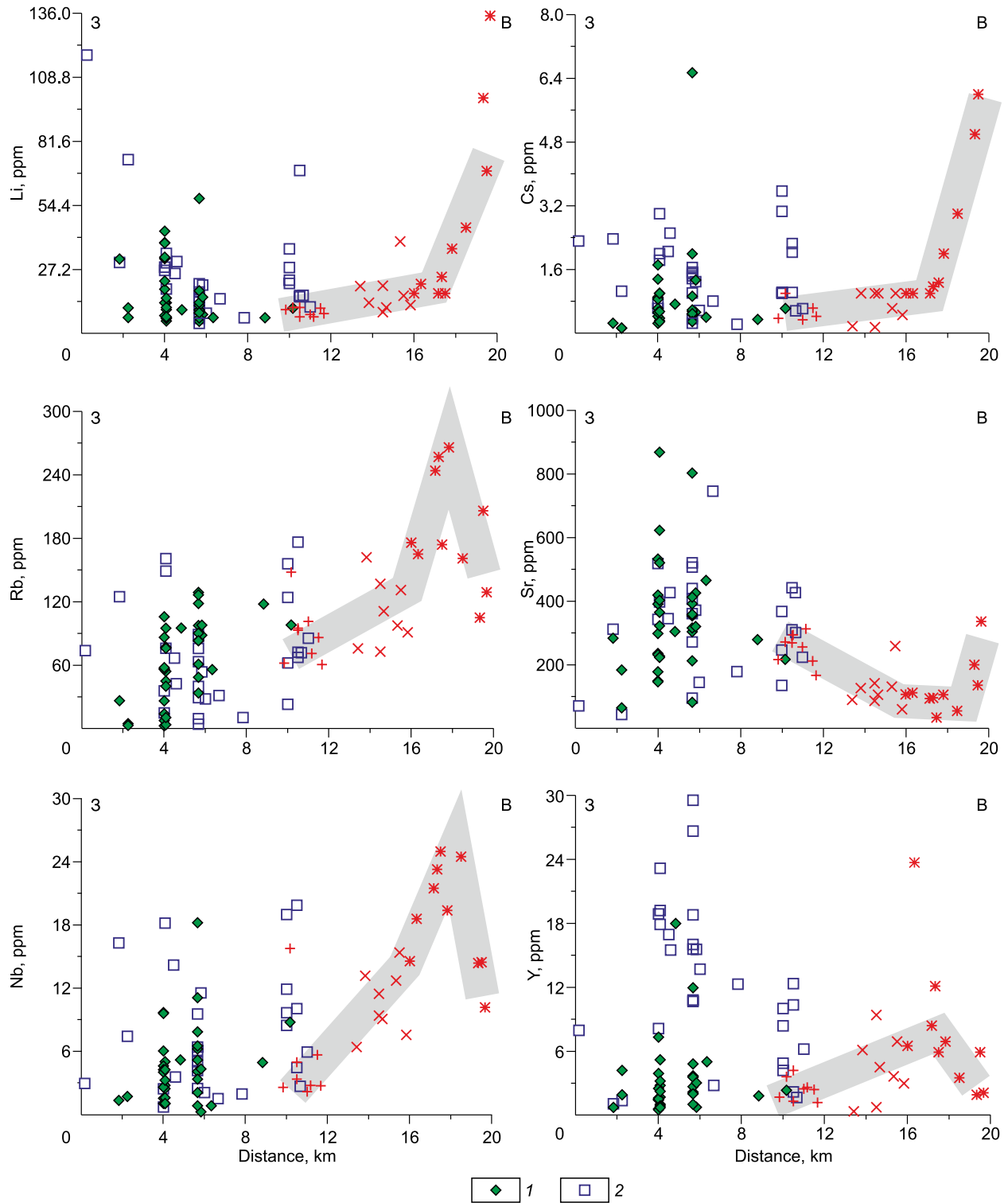


**Fig. 14.** Diagrams of distance from relative meridian vs. contents of Li, Cs, Rb, Sr, Nb, Y for granites of the Murzinka pluton (1–3, the same as in Fig. 12), vein granites of the Yuzhakovo complex (4) and gneisses (5). Solid gray line—evolutionary trend of granites of the Murzinka pluton.

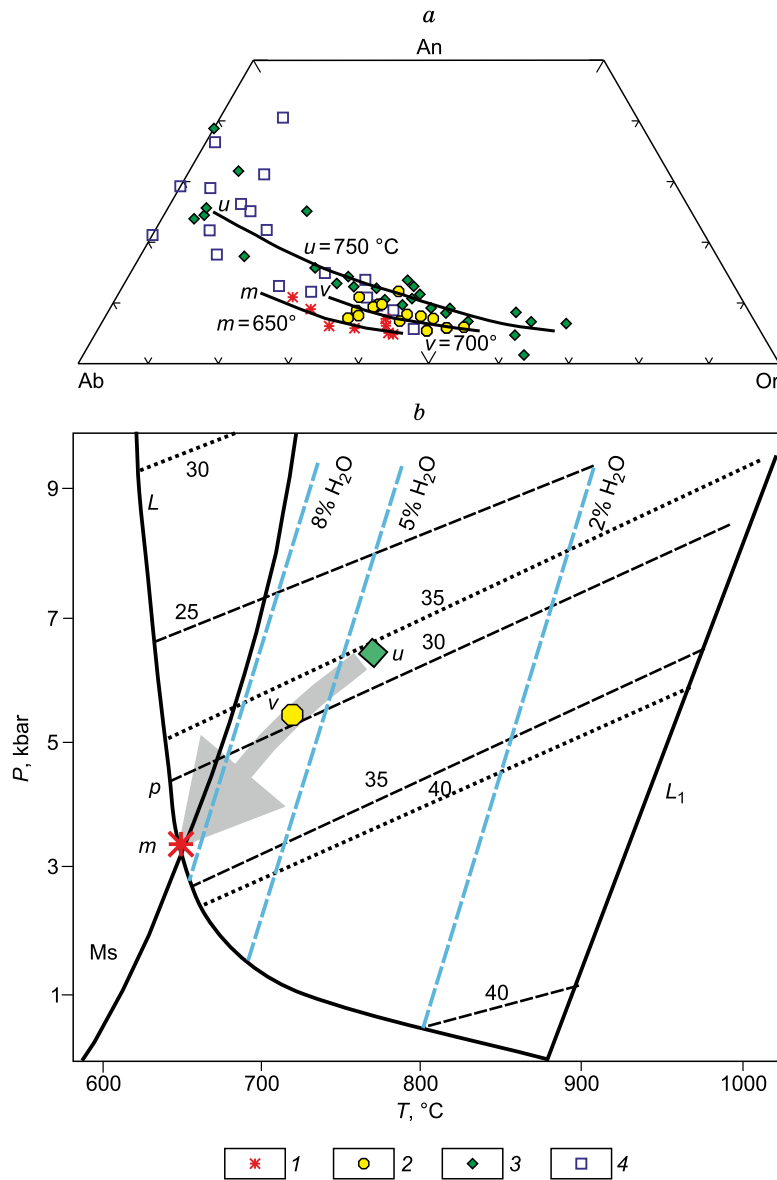


**Fig. 15.** The Ab–An–Or diagrams for granitoids and metamorphic rocks (a) and  $P$ – $T$  conditions of granite formation (b). a: 1–3, complexes of granitoids: 1, Murzinka; 2, Vatikha; 3, Yuzhakovo; 4, gneisses. Letters *m*, *v*, and *u* designate trends of corresponding complexes. These trends are associated with isotherms of homogeneity and decay of solid solutions of triple feldspars (Ribbe, 1975; and references therein). Standard quantities of Ab, An, and Or correspond to mesonorms (standard compositions, in which biotite and amphibole were recalculated instead of anhydrous iron-magnesium silicates). b. See the construction design of the diagram and sources of data in (Fershtater, 1987; Fig. 33). Supplementary explanations. Position of water-saturated ( $L$ ) and dry ( $L_1$ ) melting curves in the Ab–Q–Or– $\text{H}_2\text{O}$  system, and liquidus lines (blue dashes) for water contents of 2, 5 and 8 wt % was refined based on the data in (Johannes and Holtz, 1996; Holtz et al., 2001). Dashed lines with indices 40, 35, 30, 25—the quartz content at the ternary minimum of the Ab–Q–Or system; dotted lines—the same as in the system of Ab–Q–Or–An at  $\text{An}/(\text{An} + \text{Ab} + \text{Or}) = 0.05$ . The position of lines was also verified based on the data in (Johannes and Holtz, 1996; Holtz et al., 2001). An average quartz content in granites of the Yuzhakovo (*u*), Vatikha (*v*) and Murzinka (*m*) complexes calculated based on mesonorms. Ms, curve of muscovite stability in granite (Huang and Willie, 1973). See commentaries in text.

widespread (Fershtater, 2013). The plutons of the latter are confined to dome structures and formed as a result of diapirism together with crack propagation (Clemens and Mawer, 1992). In such plutons separate granite bodies varying in the structure and composition are predominantly flat-lying (Fershtater and Borodina, 1975).

## CONCLUSIONS

Gneisses of the Murzinka–Adui metamorphic complex and granites of the Murzinka pluton contain zircons of several age groups (from 1588 to 260 Ma), which recoded different ages of the primary crust, transformations stages of

the protolith, stages of the metamorphism of gneisses, and the formation period of vein and larger granite bodies. Granites capture zircons from gneisses. Zircons of the latter record the stages of granite formation.

Isotope–geochemical parameters of rocks of the MMC indicate a different degree of the mantle–crust interaction and their participation in the formation of rocks of the crystalline basement and the newly-formed crust. Orthogneisses of the central part of the MMC and granites of the most part of the Murzinka pluton are characterized by minimum Sr isotope ratios at maximum  $\epsilon_{Nd}$ , which is evidence of the mantle nature of the protolith. The granite veins of the Yuzhakovo complex and the western part of the Murzinka pluton have the highest values of the above parameters. It is proposed that sialic rocks of the pre-Paleozoic basement were the protolith for granite melts.

The wide variations in the chemical composition, age, and isotope parameters indicate the complicated history of formation of the interformational Murzinka granite pluton and its frame. The more detailed studies and the subsequent modelling of the processes of mantle–crustal interaction yield a complete picture of the geological evolution of this segment of the Ural orogen.

This work was performed within the framework of the research projects No. 0393-2016-0020 of the State Task of Institute of Geology and Geochemistry UB RAS (state registration No. AAAA-A18-118052590029-6) and 0393-2016-0025. This work was supported by the Program of the Presidium of the Ural Branch of the Russian Academy of Science (project No. 18-5-5-54).

## REFERENCES

- Bellavin, O.V., Aleinikov, A.L., 1968. Determination of the shape of granite plutons based on gravimetric data (on the example of the Konevo–Karas'evsky pluton, Middle Urals). *Sovetskaya Geologiya*, No. 2, 18–25.
- Clemens, J.D., Mawer, C.K., 1992. Granite magma transport by fracture propagation. *Tectonophysics* 204 (3–4), 339–360.
- Couzinie, S., Moyen, J.-F., Villaros, A., Paquett, J.-L., Scarrow, J.H., Marignac, C., 2014. Temporal relationships between Mg-K mafic magmatism and catastrophic melting of the Variscan crust in the southern part of Velay Complex (Massif Central, France). *J. Geosci.* 59, 69–86.
- Fershtater, G.B., 1987. *Petrology of the Main Intrusive Associations* [in Russian]. Nauka, Moscow.
- Fershtater, G.B. (Ed.), 1994. *Orogenic Granitoid Magmatism of the Urals* [in Russian]. IGG UrO RAN, Miass.
- Fershtater, G.B., 2013. *The Paleozoic Intrusive Magmatism in the Middle and Southern Urals* [in Russian]. Izd. UrO RAN, Yekaterinburg.
- Fershtater, G.B., Borodina, N.S., 1975. *Petrology of Magmatic Granitoids* [in Russian]. Nauka, Moscow.
- Fershtater, G.B., Borodina, N.S., Soloshenko, N.G., Streletskaia, M.V., 2015. New data on the nature of the substrate of Late Paleozoic granites of the Southern Urals. *Litosfera*, No. 3, 5–16.
- Fershtater, G.B., Borodina, N.S., Bea, F., Montero, P., 2018. Model of mantle–crustal interaction and magma generation in the suprasubduction orogen (Paleozoic of the Urals). *Litosfera*, No. 2, 177–207.
- Gerdes, A., Montero, P., Bea, F., Fershtater, G., Borodina, N., Osipova, T., Shardakova, G., 2002. Peraluminous granites frequently with mantle-like isotope compositions: the continental-type Murzinka and Dzhabyk batholiths of the eastern Urals. *Int. J. Earth Sci.* 91 (1), 3–19.
- Holtz, F., Becker, A., Freise, M., Johannes, W., 2001. The water-undersaturated and dry Qz–Ab–Or system revisited. Experimental results of very low water activities and geological implications. *Contrib. Mineral. Petrol.* 141 (3), 347–357.
- Huang, W.L., Willie, R.J., 1973. Melting relations of muscovite–granite to 35 kbar as a model for fusion of metamorphosed subducted oceanic sediments. *Contrib. Mineral. Petrol.* 42 (1) 1–14.
- Johannes, W., Holtz, F., 1996. Petrogenesis and experimental petrology of granitic rocks, in: *Minerals and Rocks*, Vol. 22. Springer, pp. 115–275.
- Kovalenko, V.Ya., Yarmolyuk, V.V., Kovach, V.P., Kotov, A.B., Kozakov, I.K., Salmikova, E.B., 1996. Sources of Phanerozoic granitoids in Central Asia: Sm–Nd isotope data. *Geokhimiya*, No. 8, 1–14.
- Krasnobaev, A.A., 1986. *Zircon as Indicator of Geological Processes* [in Russian]. Nauka, Moscow.
- Montero, P., Bea, F., Gerdes, A., Fershtater, G.B., Osipova, T.A., Borodina, N.S., Zinkova, E.A., 2000. Single-zircon evaporation ages and Rb–Sr dating of four major Variscan batholiths of the Urals: a perspective on the timing of deformation and granite generation. *Tectonophysics* 317 (1–2), 93–108.
- Petford, N., Kerr, C.R., Lister, R.G., 1993. Dike transport of granitoid magmas. *Geology* 21 (9), 845–848.
- Ribbe, P.H., 1975. *Feldspar Mineralogy: Short Course Notes*, Vol. 2. Am. Mineral. Soc. Southern Print. Co., Blacksburg, pp. 1–52.
- Sabatier, H., 1980. Vaugnerites and granites, a peculiar association of basic and acid rocks. *Bull. Mineral.* 103, 507–522.
- Sabatier, H., 1991. Vaugnerites: special lamprophyre-derived mafic enclaves in some Hercynian granites from Western and Central Europe, in: Didier, J., Barbarin, B. (Eds.), *Enclaves and Granite Petrology*. Elsevier, Amsterdam, pp. 63–81.
- Scarrow, J.H., Molina, J., Bea, F., Montero, P., 2009. Within-plate calc-alkaline rocks: insights from alkaline mafic magmas–peraluminous crustal melt hybrid appinites of the Central Iberian Variscan continental collision. *Lithos* 110 (1–4), 50–64.
- Shardakova, G.Yu., 2016. Granitoids of the Ufaiei block: geodynamic settings, age, sources, problems. *Litosfera*, No. 4, 133–137.
- Slabunov, A.I., Lobach-Zhuchenko, S.B., Bibikova, E.V., Balaganskii, V.V., Sorjonen-Ward, P., Volodichev, O.I., Shchipansky, A.V., Svetov, S.A., Chekulaev, V.P., Arestova, N.A., Stepanov, V.S., 2006. The Archean of the Baltic Shield: geology, geochronology, and geodynamic settings. *Geotectonics* 40 (6), 409–433.
- Trifonov, V.P., Vlokh, N.P., Aleinikov, A.L., Bellavin, O.V., Zubkov, A.V., 1968. Phenomena of the squeezing of granite plutons. *Dokl. Akad. Nauk SSSR* 179 (1), 69–170.
- Tsygankov, A.A., 2014. Late Paleozoic granitoids in western Transbaikalia: sequence of formation, sources of magma, and geodynamics. *Russian Geology and Geophysics (Geologiya i Geofizika)* 55 (2), 153–176 (197–227).
- Vishnyakova, M.D., Borodina, N.S., Fershtater, G.B., Bea, F., Montero, P., 2017. U–Pb zircon age of rocks of the Krutikha pluton as a possible protolith of some granites of the Adui pluton (Middle Urals), in: *Yearbook-2016 (Trans. IGG UrO RAN)* [in Russian]. UrO RAN, Yekaterinburg, pp. 260–263.
- Yarmolyuk, V.V., Kovalenko, V.I., 2003. Batholiths and geodynamics of batholith formation in the Central Asian fold belt. *Geologiya i Geofizika (Russian Geology and Geophysics)* 44 (12), 1305–1320 (1260–1274).